Quaternary Science Reviews 30 (2011) 2551–2569

Contents lists available at ScienceDirect

Quaternary Science Reviews

journal homepage: www.elsevier.com/locate/quascirev

Radiocarbon chronology of the late-glacial Puerto Bandera moraines, Southern Patagonian Icefield, Argentina

J.A. Strelin [a,*], G.H. Denton [b], M.J. Vandergoes [c], U.S. Ninnemann [d,e], A.E. Putnam [b]

[a] CICTERRA Universidad Nacional de Córdoba, Instituto Antártico Argentino, Avda. Vélez Sarsfield 1611, X5016GCA, Córdoba, Argentina
[b] Department of Earth Sciences and Climate Change Institute, University of Maine, Orono, ME 04469, USA
[c] GNS Science, Lower Hutt, New Zealand
[d] Bjerknes Centre for Climate Research, University of Bergen, Allégaten 55, 5007 Bergen, Norway
[e] Department of Earth Science, University of Bergen, Allégaten 41, N-5007 Bergen, Norway

ARTICLE INFO

Article history:
Received 26 October 2010
Received in revised form
25 April 2011
Accepted 5 May 2011
Available online 30 July 2011

Keywords:
Late-glacial
Termination
Radiocarbon
Glacier
Chronology
Patagonia
Southern Patagonian
Icefield
Sea-surface temperature
Antarctic cold reversal
Younger Dryas
Deglaciation

ABSTRACT

We report radiocarbon dates that constrain the timing of the deposition of the late-glacial Puerto Bandera moraine system alongside the western reaches of Lago Argentino adjacent to the Southern Patagonian Icefield. Close maximum-limiting radiocarbon ages ($n = 11$) for glacier advance into the outer moraines, with a mean value of 11,100 ± 60 ^{14}C yrs BP (12,990 ± 80 cal yrs BP), were obtained from wood in deformation (soft) till exposed beneath flow and lodgment till in Bahía del Quemado on the northeast side of Brazo Norte (North Branch) of western Lago Argentino. Other exposures of this basal deformation till in Bahía del Quemado reveal incorporated clasts of peat, along with larger inclusions of deformed glaciofluvial and lacustrine deposits. Radiocarbon dates of wood included in these reworked peat clasts range from 11,450 ± 45 ^{14}C yrs BP to 13,450 ± 150 ^{14}C yrs BP (13,315 ± 60 to 16,440 ± 340 cal yrs BP). The implication is that, during this interval, glacier fronts were situated inboard of the Puerto Bandera moraines, with the peat clasts and larger proglacial deposits being eroded and then included in the basal till during the Puerto Bandera advance.

Minimum-limiting radiocarbon ages for ice retreat come from basal peat in cores sampled in spillways and depressions generated during abandonment of the Puerto Bandera moraines. Glacier recession and subsequent plant colonization were initiated close behind different frontal sectors of these moraines prior to: 10,750 ± 75 ^{14}C yrs BP (12,660 ± 70 cal yrs BP) east of Brazo Rico, 10,550 ± 55 ^{14}C yrs BP (12,490 ± 80 cal yrs BP) in Peninsula Avellaneda, and 10,400 ± 50 ^{14}C yrs BP (12,280 ± 110 cal yrs BP) in Bahía Catalana. In addition, a radiocarbon date indicates that by 10,350 ± 45 ^{14}C yrs BP (12,220 ± 110 cal yrs BP), the Brazo Norte lobe (or former Upsala Glacier) had receded well up the northern branch of Lago Argentino, to a position behind the Herminita moraines. Furthermore, glacier termini had receded to just outboard of the outer Holocene moraines at Lago Frías and Lago Pearson (Anita) prior to 10,400 ± 40 ^{14}C yrs BP (12,270 ± 100 cal yrs BP) and 9040 ± 45 ^{14}C yrs BP (10,210 ± 50 cal yrs BP), respectively. The most extensive recession registered during the early Holocene was in Agassiz Este Valley, where the Upsala Glacier had pulled back behind the outer Holocene moraine, reaching close to the present-day glacier terminus before 8290 ± 40 ^{14}C yrs BP (9300 ± 80 cal yrs BP).

The radiocarbon-dated fluctuations of the Lago Argentino glacier in late-glacial time, given here, are in accord with changes in ocean mixed layer properties, predominately temperature, derived from the isotopic record given here of ODP Core 1233, taken a short distance off shore of the Chilean Lake District. It also matches recently published chronologies of late-glacial moraines in the Southern Alps of New Zealand on the opposite side of the Pacific Ocean from Lago Argentino. Finally, the timing of the late-glacial reversal of the Lago Argentino glacier fits the most recent chronology for the culmination of the Antarctic Cold Reversal (ACR) in the deuterium record of the EPICA Dome C ice core from high on the East Antarctic Plateau. Therefore, we conclude that the climate signature of the ACR was widespread in both the ocean and the atmosphere over at least the southern quarter of the globe.

* Corresponding author.
E-mail address: jstrelin@yahoo.com.ar (J.A. Strelin).

0277-3791/$ – see front matter © 2011 Elsevier Ltd. All rights reserved.
doi:10.1016/j.quascirev.2011.05.004

1. Introduction

During the last termination millennial-scale climate changes are thought to have played a central role in propelling Earth's climate from ice age to interglacial conditions (Denton et al., 2010). And yet both the geographical extent and the signature of such climate changes remain uncertain because well-resolved terrestrial records of late-glacial climate are sparse in the Southern Hemisphere. In particular, the signature of Patagonian climate change during the late-glacial period remains unresolved (see Rodbell et al., 2010 for a review of available records). Based on glacial stratigraphy, moraine geomorphology, and radiocarbon dating, we present here a new record of late-glacial fluctuations of the eastern margin of the South Patagonian Icefield in the Lago Argentino area of the southern Andes. The glaciated Patagonian Andes transect the core latitudes of the southern westerly wind belt, intercept the frontal boundary between the South Pacific and Southern Oceans (the 'Subtropical Front' or 'STF', following Sikes et al., 2009), and are close to a major center of Antarctic Intermediate Water (AAIW) formation. Thus glaciers of the Patagonian Andes are well situated for monitoring millennial-scale climate changes near the northern margin of the Southern Ocean.

Caldenius (1932), Feruglio (1944), and Mercer (1976) provided the first descriptions of moraine distribution and chronology for the eastern slope of Cordillera Patagónica near Lago Argentino. Several subsequent field studies were carried out to improve the knowledge of glacier episodes in this region. Paleomagnetic dating (Mörner and Sylwan, 1989) and isotopic ages (Mercer et al., 1975; Singer et al., 2004) were applied to bracket the older glaciations, whereas the radiocarbon method, by measuring mainly minimum ages for glacial events, was used to determine the Last Glaciation and Holocene glacier chronology (Mercer, 1965, 1970; 1976; Mercer and Ager, 1983). The lack of organic samples, due to the arid climate that prevails east of Cordillera Patagónica, makes it difficult to achieve an acceptable radiocarbon chronology of glacial deposits. Cosmogenic exposure dating has also been applied to the Pleistocene moraines on the eastern precordilleran slope (Kaplan et al., 2004, 2005; Ackert et al., 2008). It follows from these chronological and additional detailed morphostratigraphic studies (Malagnino, 1995; Strelin and Malagnino, 1996) that the southern Patagonian extra-Andean region was reached at least five times by Andean glacier lobes between the late Miocene and the late Pleistocene. It is also generally accepted that the prominent moraine belts that enclose the major Patagonian lakes represent the Last Glacial Maximum (LGM), but there is significant controversy concerning the occurrence and timing of late-glacial and subsequent advances.

In studies carried out between Lago Pueyrredón and Lago Viedma (Fig. 1), a marked shrinkage (reaching close to the Holocene moraines) of the glaciers on both cordilleran slopes during the late-glacial, particularly during the European Younger Dryas chronozone, was proposed (Mercer, 1976; Roethlisberger, 1986; McCulloch et al., 2000). Conversely, a relatively important late-glacial (including Younger Dryas) advance of the Lago Pueyrredón, Lago San Martín and Lago Viedma glacier lobes, reaching Caldenius (1932) finiglacial moraine limit, was suggested by Wenzens (2002). Wenzens (2002) argued that Caldenius's (1932) finiglacial ice limit included three late-glacial substades, with the oldest taking place before 13,000 ^{14}C yrs BP, the second before 11,800 ^{14}C yrs BP, and the last before 9590 and 9480 ^{14}C yrs BP.

At Lago Argentino (Fig. 1), the late-glacial Puerto Bandera glaciers reached the western sector of the lake, depositing the Puerto Bandera moraines (Figs. 2 and 3). Strelin and Denton (2005) gave a close maximum-limiting radiocarbon age of 11,170 ± 100 ^{14}C yrs BP and a minimum-limiting age of 10,390 ^{14}C yrs BP for deposition of the Puerto Bandera moraines; this chronology is roughly in accord with Caldenius's (1932) proposed finiglacial age. In sharp contrast with the chronology of Strelin and Denton (2005), Ackert et al. (2008) proposed an early Holocene age (10,800 ± 500 yrs)

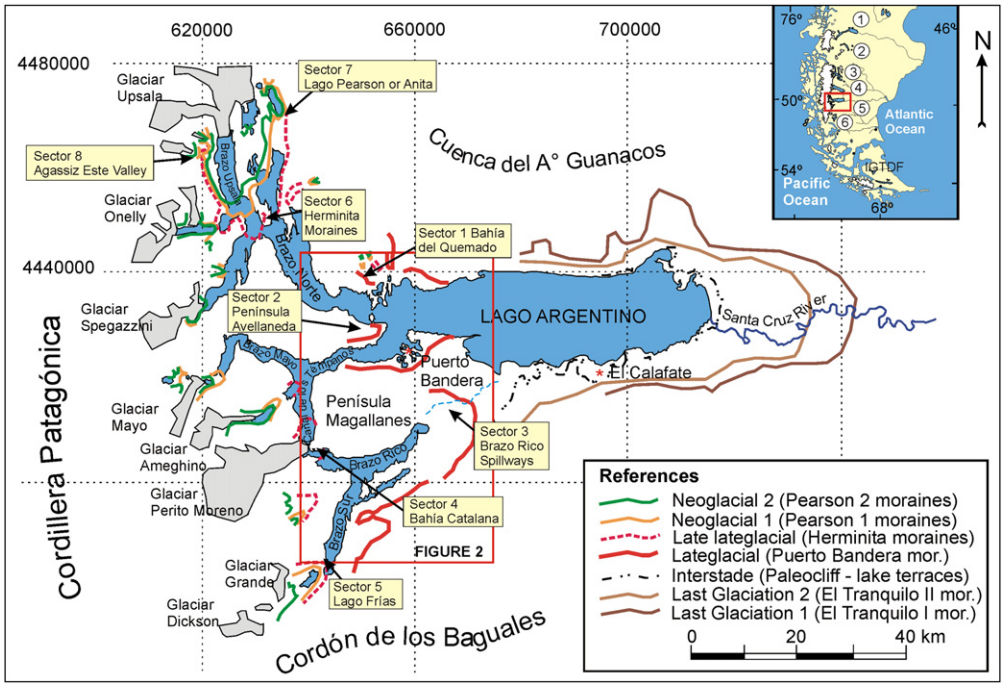

Fig. 1. Location map using UTM projection. Last Glaciation El Tranquilo moraines, late-glacial Puerto Bandera moraines (PB1 in Fig. 2), and Neoglacial moraines in Lago Argentino basin. The specific sectors mentioned in the text are shown on this map. In the southern South America reference map (top-right): 1) Lago Buenos Aires-General Carreras, 2) Lago Pueyrredón-Cochrane, 3) Lago san Martín-O'Higgins, 4) Lago Viedma, 5) Lago Argentino, 6) Torres del Paine region, IGTF = Isla Grande de Tierra del Fuego.

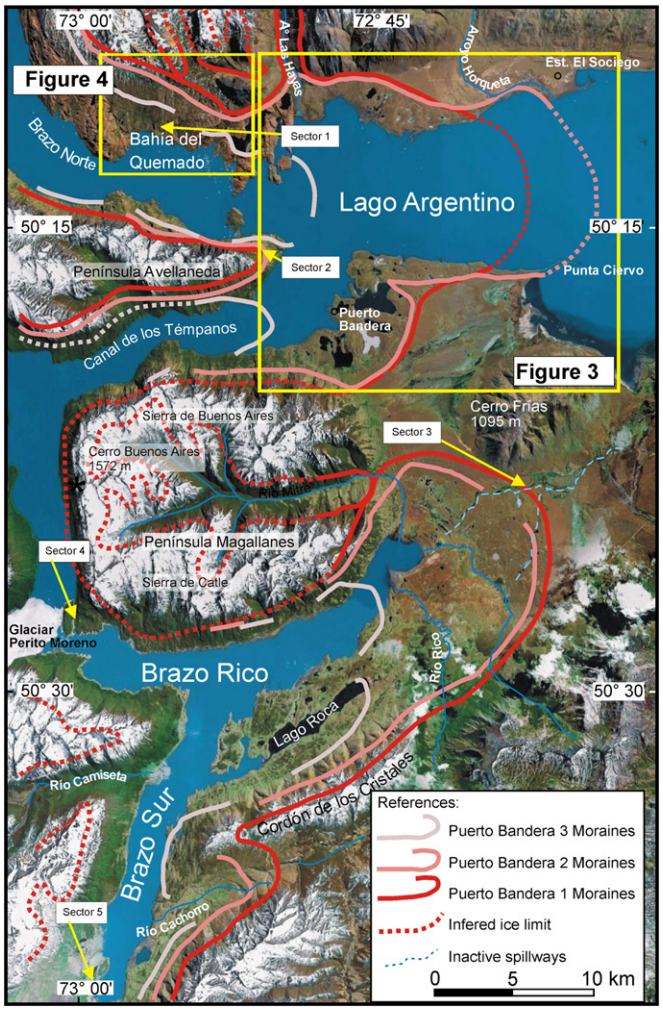

Fig. 2. Late-glacial Puerto Bandera moraines in the western reaches of Lago Argentino.

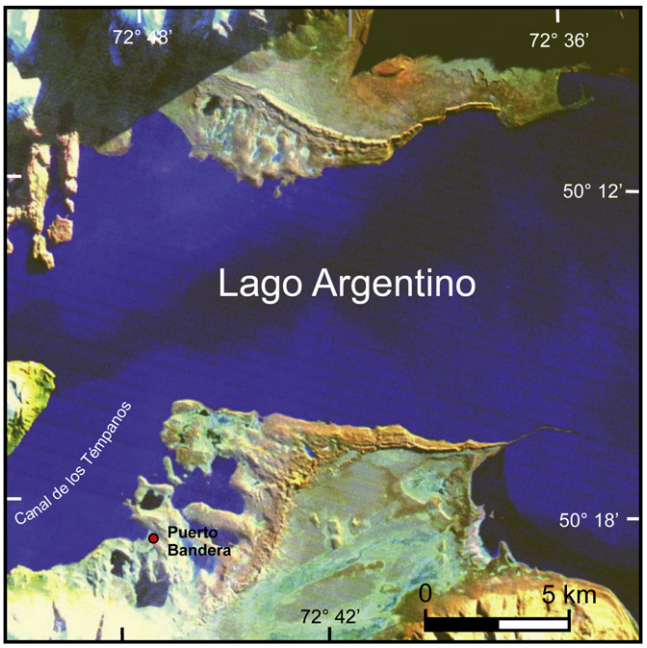

Fig. 3. Satellite image showing the Puerto Bandera moraines alongside Brazo Norte and Canal de los Témpanos in western Lago Argentino. The left-lateral moraines are at the top of the images, whereas the right laterals are at the bottom. The position of this image is depicted in Fig. 2.

for the Puerto Bandera moraines on the basis of cosmogenic ^{10}Be exposure dating.

It is widely accepted that the chronology of the Puerto Bandera moraines is a key for deciphering the late-glacial history of southern Patagonia (Mercer, 1968, 1970; 1976). Therefore, we attempted to improve the geomorphologic, stratigraphic, and chronologic basis for interpretation of these moraines. As a result of our recent field work in the western branches of Lago Argentino, we are now able to present numerous radiocarbon dates to confine the depositional history of the Puerto Bandera moraines, as well as of the intervals of retreat before and after emplacement of the moraines. New radiocarbon dates provided in this paper are expressed with the 1σ error in the text. Corresponding calibrated ages are reported with 1σ error. All dates, including the 2σ calibrated range, are listed in the tables.

2. Physical setting

Lago Argentino is located in the transitional zone between the Cordillera Patagónica and the Andean foothills (Fig. 1). According to Riccardi and Rolleri (1980), the area includes upper Jurassic silicic-volcanic and marine-to-continental sedimentary rocks formed during the Gondwana rifting, as well as volcaniclastic turbidites and ophiolite successions of the Lower Cretaceous Rocas Verdes Marginal Basin. The Precordillera is composed of Lower Cretaceous to Tertiary marine-to-continental sedimentary rocks of the Austral (Magallanes) Foreland Basin. The axis of the Central Cordillera, located immediately west of Lago Argentino, consists of a Gondwana Paleozoic metamorphic terrain made up of schists, silicic-volcanics, and volcaniclastic assemblages that are injected by Cretaceous to Cenozoic plutonic, largely granitic, rocks. The uplift, folding and thrusting of Cordillera Patagónica occurred during several Late Cretaceous to Cenozoic Andean orogenic phases. The resulting north-south folds and faults controlled the landscape development.

During at least five major glaciations of Late Cenozoic time, Andean ice expanded eastward to the extra-Andean domain, contributing to the shaping of the Lago Argentino-Upper Santa Cruz River Valley. The last glaciation involved two significant advances of glaciers that overrode the eastern edge of the main water body of Lago Argentino and deposited two large and complex moraine arcs: El Tranquilo I and El Tranquilo II (Strelin and Malagnino, 1996). Hulton et al. (2002) postulated that during this glacier advance the mean air temperature was 6 °C below that of the present. Reworked glaciogenic deposits of the El Tranquilo II moraines dam the present-day lake. Several recessional moraines as well as ice-marginal and glaciofluvial terraces were formed during glacier retreat. The glacial lake that occupied the ice-excavated depression behind the El Tranquilo moraines eroded several terraces during the Río Santa Cruz entrenchment (Strelin and Malagnino, 1996). A late-glacial advance reached the western part of the main body of Lago Argentino, resulting in the deposition of the well-preserved Puerto Bandera moraines, together with outwash and ice-contact terraces (Strelin and Malagnino, 2000).

A deeply entrenched cordilleran and precordilleran topographic relief was exposed during the Holocene, when the outlet glaciers receded deep into the cordilleran valleys. Since then, there have occurred only relatively restricted Neoglacial advances that resulted in minor glaciogenic landforms (Mercer, 1965; Malagnino and Strelin, 1992).

The Southern Patagonian Icefield remains as a remnant of the last ice age. It covers the continental divide over an area of about

13,000 km^2, reaching mean and maximum altitudes of ca. 1600 and 3500 m a.s.l. respectively (Casassa et al., 2000).

As in all of the Cordillera Patagónica, the climate of Lago Argentino is related to the interaction between the persistent westerlies and the Andes. Water-saturated air masses that reach the western cordilleran slope produce an extreme oceanic climate, with high cloudiness and annual precipitation peaking at about 10,000 mm on the upper part of the SPI (Casassa and Rivera, 1999). Further eastward in the Cordillera, the climate becomes dryer, yielding at El Calafate (about 72° W) only 200 mm of annual precipitation (Servicio Meteorológico Nacional). There are no air temperature data from the SPI. At the foot of the mountain area the mean annual air temperature reaches ca. 6 °C (Carrasco et al., 1998). Under these climatic conditions the glaciers enter the Pacific fiords on the western cordilleran slope, whereas on the eastern side only a few large glaciers now reach the inner branches of Lago Argentino (185 m a.s.l.). Judging by the excellent preservation of many old landforms of the eastern sub-Andean region, dry climate conditions have been prevalent here since before the Pleistocene (Strelin and Malagnino, 1996).

During the Holocene vegetation colonized deglaciated landscapes, with ecotone distribution strongly controlled by topography, local lapse rate, and westerly air mass circulation. Because of the climate conditions, wetlands (patches of peat bogs), Nothofagus evergreen, and/or Nothofagus deciduous forests occupy cordilleran valleys west of the icefield. On the eastern cordilleran side of the Icefield, tree line reaches about 1000 m (a.s.l). Andean tundra

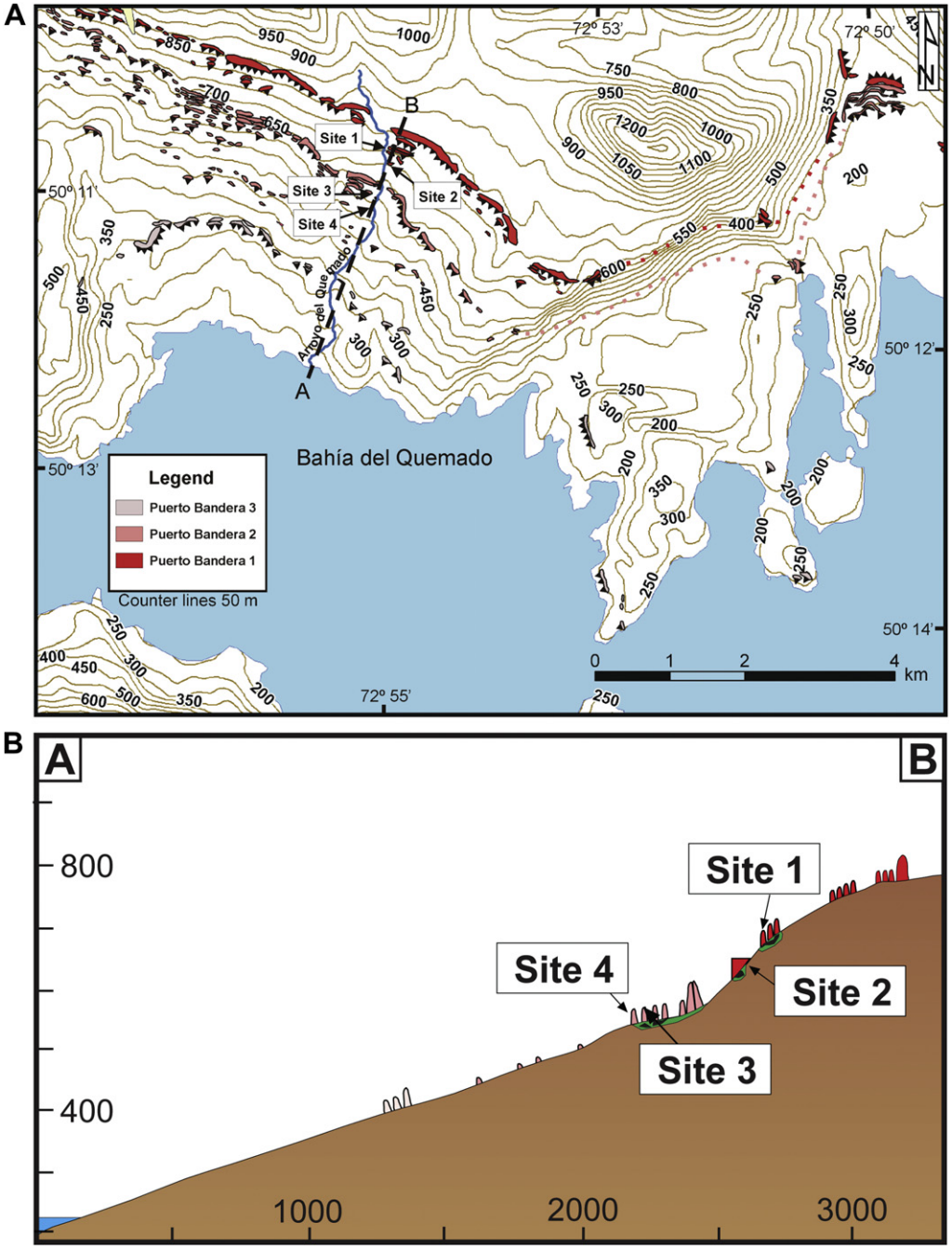

Fig. 4. (A) Bahía del Quemado Geomorphic map showing PB1, PB2 and PB3 moraine groups (ticks on ice-proximal side). Arroyo del Quemado topographic section AB and exposure sites 1 to 4 are indicated. (B) Topographic section through PB moraines showing the different moraine ridges and exposure sites of Figs. 6–9.

develops on the upper slopes and the ELA is located about 1300 m a.s.l., which is 300–500 m higher than on the west side (Casassa et al., 2000). The precipitation diminishes rapidly from west to east leading to a narrow vegetation transitional zone (ecotone) along 73° W, where forests give way to the Patagonian steppe. It is this ecotonal zone, which coincides roughly with the Cordillera - Precordillera boundary, where our research work was undertaken.

3. Methodology

Between March 2004 and April 2008, five field excursions were undertaken for detailed study of the Puerto Bandera moraines. Fig. 1 shows the prime sectors where field studies were carried out and where most samples for radiocarbon dating were collected.

Sector 1. Bahía del Quemado, where exposures in Puerto Bandera lateral moraines were discovered in November 1997.

Sector 2. Península Avellaneda, where peat bogs are situated between and behind the interlobate Puerto Bandera moraine.

Sector 3. Brazo Rico, where two spillways of a proglacial lake cross the Puerto Bandera moraines immediately south of Cerro Frías; the youngest of the two spillways was first studied by Mercer (1968) and by Allen Ashworth (personal communication, 2005).

Sector 4. Bahía Catalana peat bog, occupying a former channel that discharges melt waters from the retreating Brazo Rico Glacier into Canal de los Témpanos. This peat bog was previously sampled and dated by Mercer and Ager (1983) and by Allen Ashworth (personal communication, 2005).

Sector 5. Lago Frías, where a peat bog is located in front of the outer Holocene moraines.

Sector 6. Península Herminita, where peat bogs are situated between and inboard of Herminita moraines.

Sector 7. Lago Pearson (Anita), where peat bogs occur in front of the outer Holocene moraines.

Sector 8. Agassiz Este Valley, where exposures appear cut through a shared moraine complex formed by the coalescence of Agassiz Este Glacier and a lateral lobe of Upsala Glacier.

In sectors 1 and 8 detailed stratigraphic profiles were described using facies identification based on texture, fabric, composition, sedimentary structures, and stratigraphic relationships. These parameters are used to determine sedimentary processes (mostly glaciogenic) and to track the probable glacial behavior. Peat clasts and larger inclusions discovered in some of the deposits contain twigs and pieces of wood that were sampled for radiocarbon dating.

In sectors 2 to 7, peat cores were obtained in bogs and spillways located behind and crossing the late-glacial moraine ridges. The cores were logged for their stratigraphy and subsampled for basal organic material for radiocarbon dating. The radiocarbon samples comprised pieces of twigs, wood, bark, seeds, sedge, and plants picked out from bulk peat inclusions, soil horizons, and organic layers.

All the samples were collected between 2004 and 2008 and were dated by AMS in NOSAMS at the Woods Hole Oceanographic Institution. Mean ± 1 sigma calendar ages were determined using OxCal 4.1.5 software (Bronk Ramsay, 2010) and the IntCal09 curve of Reimer et al. (2009).

Tephrochronological and cosmogenic isotope studies are in progress.

Topographic maps (1:100,000; Instituto Geográfico Nacional, Argentina), air photographs (1:70,000; Instituto Geográfico Nacional, Argentina), and satellite scenes (30–15 m LANDSAT TM; Eros data center, USA) were used to draw several of the figures.

4. The Puerto Bandera moraines

Eight main outlet glaciers now drain from the Southern Patagonian Icefield into the western reaches of the Lago Argentino basin. At the Last Glaciation, these glaciers coalesced to send a large ice tongue eastward through the lake basin to the position of the El Tranquilo moraines (Fig. 1). The subsequent ice recession westward back through Lago Argentino was interrupted by a readvance to the spectacular Puerto Bandera moraine system (Strelin and Malagnino, 2000). By the time of this readvance, the main glacial tongue had divided into four lobes separated by Peninsula Avellaneda, Península Magallanes, and Cordón de los Cristales (Figs. 1 and 2). The southern three lobes terminated on land, whereas the northern lobe calved into Lago Argentino. Overall, the Puerto Bandera (PB) moraines register three closely spaced ice-marginal pulses: Puerto Bandera 1 (PB1, oldest), Puerto Bandera 2 (PB2, middle), and Puerto Bandera 3 (PB3, youngest) (Fig. 2). The separation of these pulses follows geomorphological considerations, i.e. the grouping of several tightly packed moraine ridges behind a prominent continuous moraine ridge. In the case of the right lateral moraine belt occurring alongside the southern shore of Lago Argentino, the PB2 moraine appears to truncate the older PB1 moraines.

4.1. Post-LGM ice recession and maximum-limiting ages of the Puerto Bandera moraines

The chronology of the PB moraines comes from radiocarbon samples collected at several key locations. The maximum-limiting radiocarbon ages were obtained from samples collected alongside Bahía del Quemado on the north shore of Lago Argentino (Fig. 4). Here a complex of PB lateral moraines extends along the valley at 500 m elevation above the Brazo Norte (North Branch) of the lake, which is about 800 m deep. Thus the glacier tongue was about 1300 m thick when it stood at the uppermost PB moraine above Bahía del Quemado.

Arroyo del Quemado, a small creek that flows down the northeast valley slope adjacent to Bahía del Quemado, has eroded several exposures through the PB moraine ridges. Four of these outcrops (Figs. 6–9) afford valuable radiocarbon samples that yielded maximum-limiting ages for deposition of the PB moraines (Strelin and Denton, 2005).

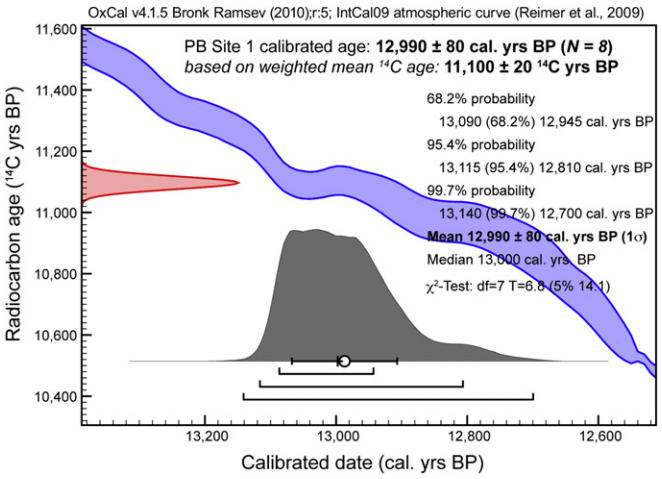

Fig. 5. Radiocarbon calendar-year conversion output for samples from PB Site 1. We employed the R_Combine component of OxCal program version 4.1.5 (Bronk Ramsay, 2010) and the IntCal09 curve of Reimer et al. (2009). Red curve plotted along vertical axis is distribution of samples ($n = 8$) in radiocarbon years. Gray curve plotted along horizontal axis shows calibration output with units expressed in 'cal. yrs BP' (i.e., calendar years before C.E. 1950). Blue area is IntCal09 calibration curve. Summary statistics are inset. Age printed in bold is the arithmetic mean with 1σ age uncertainty.

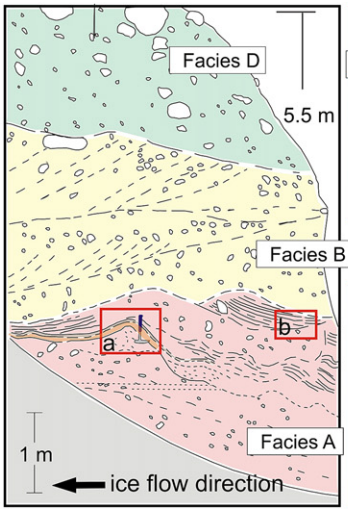

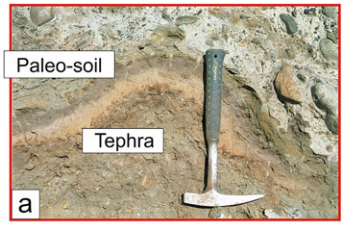

Paleo-soil

^{14}C Lab #	^{14}C age	+/- 1σ	Cal ys	+/−1σ
OS-37395	11,150	75	13,020	110
OS-37580	11,100	55	12,980	100
OS-61893	11,100	55	12,980	100
OS-63544	11,000	60	12,880	110

Sandy rhythmite

^{14}C Lab #	^{14}C age	+/- 1σ	Cal ys	+/−1σ
OS-39169	11,100	40	12,980	90
OS-39170	11,200	60	13,090	100
OS-41104	11,100	120	12,970	140
OS-68695	11,050	55	12,930	110

Fig. 6. Site 1 in section AB of Fig. 4. Outcrop located on the left (facing downstream) side of Arroyo del Quemado. View is toward the southeast. The stacked moraine ridge shows a basal deformation till that includes (a) an incipient soil developed on a thin tephra layer and (b) glaciofluvial and glaciolacustrine deposits. Pieces of twigs (c) are included in the paleosoil and sandy rhythmite, with a mean ($n = 8$) age of 11,100 ± 60 ^{14}C yrs BP (12,990 ± 80 cal yrs BP). Both the paleosoil and sandy rhythmite were generated very close in time and provide together the maximum-limiting age for PB1 moraine deposition.

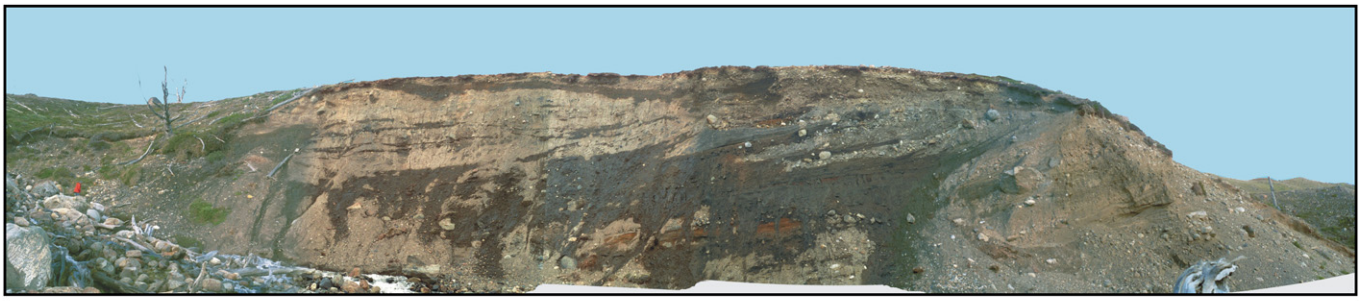

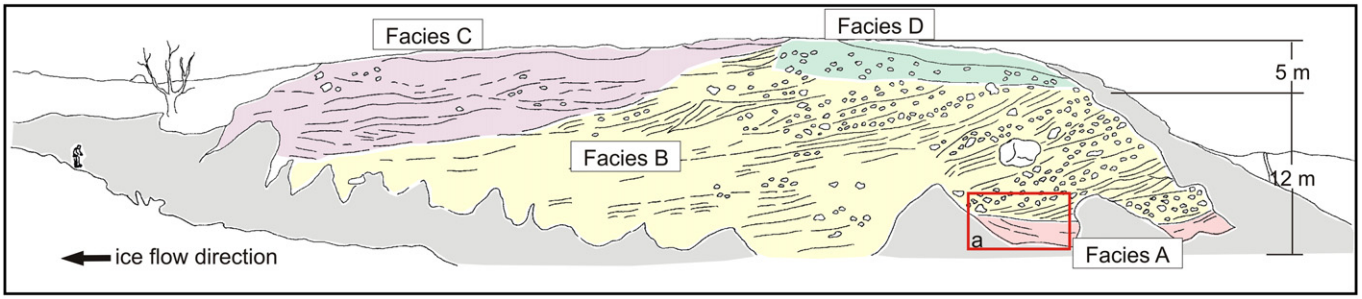

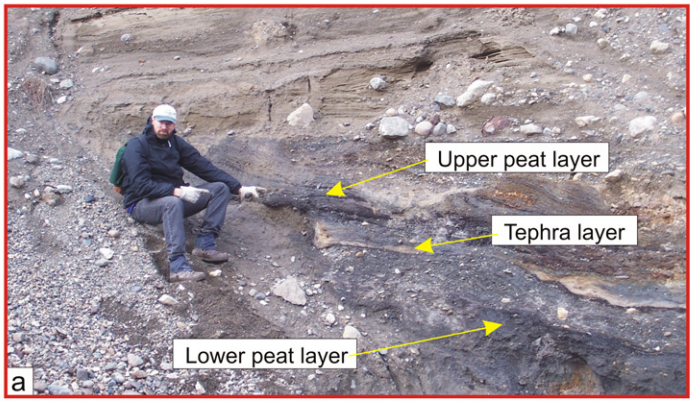

Upper peat layer

^{14}C Lab #	^{14}C age	+/-1σ	Cal ys	+/-1σ
OS-61894	12,350	55	14,410	230
OS-63568	12,300	50	14,300	225
OS-63569	12,200	55	14,070	140
OS-68696	12,150	50	14,000	90

Lower peat layer

^{14}C Lab #	^{14}C age	+/-1σ	Cal ys	+/-1σ
OS-61895	13,450	150	16,440	340
OS-63545	12,900	80	15,490	300
OS-63458	13,000	55	15,660	320
OS-68697	12,800	50	15,260	210

Fig. 7. Site 2 in section AB of Fig. 4. Outcrop located on the left (facing downstream) side of Arroyo del Quemado. View is toward the southeast. PB 1 ice-contact deposits cover a deformation till that incorporates an inclusion of well-preserved glaciofluvial sediments interlayered with tephra and peat that antedate deposition of the PB moraine.

Peat clasts

^{14}C Lab #	^{14}C age	+/- 1σ	Cal ys	+/-1σ
OS-56399	11,450	70	13,310	70
OS-56400	11,550	55	13,400	70
OS-61896	11,450	45	13,320	60

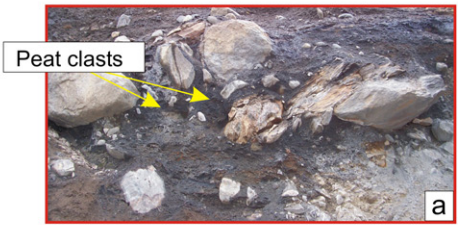

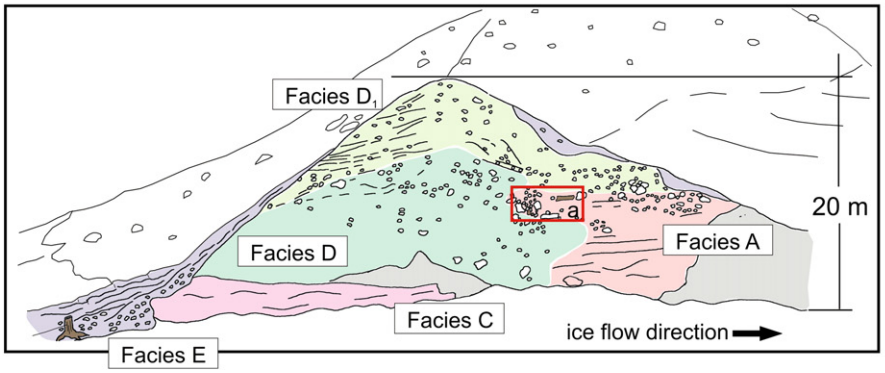

OS-61896

Fig. 8. Site 3 in section AB of Fig. 4. Outcrop located on the right side (facing downstream) of Arroyo del Quemado. View is toward the northwest. Basal glaciolacustrine and glaciofluvial deposits underlie and are partially incorporated into the sixth PB2 moraine ridge, counting down the slope from the outermost PB2 moraine. Peat clasts (a) embedded in the lodgment till incorporate twigs (b) that afford a maximum age of 11,450 ± 70 ^{14}C yrs BP (13,310 ± 70 cal yrs BP) for the accumulation of this stacked moraine ridge.

Peat clasts

^{14}C Lab #	^{14}C age	+/- 1σ	Cal ys	+/-1σ
OS-34458	13,050	45	15,760	330
OS-34460	12,750	50	15,150	190
OS-34461	13,200	45	16,080	320
OS-37396	13,250	90	16,150	350
OS-37397	13,250	75	16,170	340
OS-37131	12,950	75	15,580	320
OS-39171	13,150	50	15,970	330
OS-39172	13,300	50	16,310	300
OS-39173	13,050	50	15,760	330

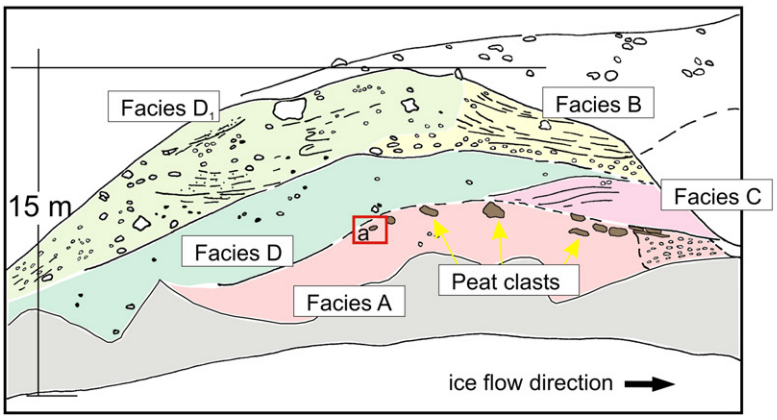

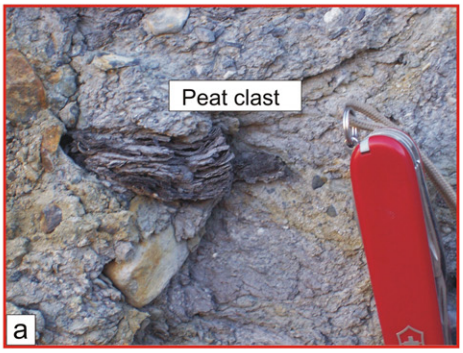

Fig. 9. Site 4 in section AB of Fig. 4. Outcrop located on the right side (facing downstream) of Arroyo del Quemado. View is toward the northwest. Many peat clasts, and one large glaciofluvial inclusion, are reworked into the basal deformation till (facies A), affording radiocarbon dates that constrain a period of ice recession prior to deposition of the PB moraines. Lodgment tills (facies D and D_1) and glaciofluvial deposits (facies C) were laid down on the basal deformation till.

The stratigraphy exposed in the moraine ridges by Arroyo del Quemado, together with the radiocarbon sample sites, are presented in Figs. 6–9. Descriptions and interpretations of lithofacies are discussed in Appendix A.

The first (oldest) PB1 moraine ridge, which rises 20 m above the surrounding terrain, is dissected by Arroyo del Quemado at 740 m a.s.l. (555 m above the lake level). Farther down the slope, which here dips toward the lake at about 12°, many recessional moraine ridges are also crossed by the arroyo. The eleventh (counting down the slope from the outermost PB1 moraine) of these recessional PB1 moraine ridges is deeply eroded by the arroyo, revealing the exposure illustrated in Fig. 6. This outcrop exposes a paleosoil and a volcanic ash that were incorporated into a deformation till (facies A), which, in turn, is overlain by about 3 m of flow and lodgment tills (facies B and D, respectively). The flow tills seal off and preserve the deformation till. Although the paleosoil and volcanic ash were slightly deformed during incorporation into the deformation till, they are intact and very close to being in place. Therefore, the radiocarbon dates of twigs included in the upper surface of the paleosoil, as well as in a sandy rhythmite that covers the soil horizon, afford a close maximum-limiting age of 11,100 ± 60 ^{14}C yrs BP (12,990 ± 80 cal yrs BP) ($n = 8$) for overriding of this site by advancing PB ice (Fig. 5).

Downslope from Site 1, the valley topography becomes a little more even than is the case higher on the slope. At a location 615 m a.s.l. (430 m above lake level), Arroyo del Quemado carved a short gully that exposes outcrops of glaciogenic sediments. The largest outcrop consists of a proximal glacial sequence, piled up into a kame terrace (Fig. 7). The basal facies in this section consists of deformation till that incorporates a large, reworked peat-tephra-glaciofluvial inclusion (facies A in Fig. 7). This inclusion represents peat that grew somewhere downslope of Site 2 for the entire interval between 13,450 ± 150 and 12,150 ± 50 ^{14}C yrs BP (16,440 ± 340 and 14,000 ± 90 cal yrs BP), and then was deposited as a reworked clast in facies A. An ocher-colored tephra layer occurs between this old peat and adjacent gravelly layers. Whether this tephra layer correlates with the tephra deposit in Site 1 is chronologically unclear. Cross-bedded glaciofluvial sands and gravels (facies C), ice-proximal flow tills (facies B), and lodgment till (facies D) accumulated into a 10-m-thick deposit. The top of this section is crowned by a subhorizontal glaciofluvial ice-proximal deposit (facies C).

Approximately 100 m downslope of Site 2 (Fig. 4A and B), the highest and outermost prominent ridge of the PB2 lateral moraine belt is crossed by the arroyo, without any exposures. Farther downslope, at Site 3, the river eroded through the sixth PB2 moraine ridge (Fig. 8), exposing a basal, slightly deformed glaciofluvial and lacustrine (rhythmite) deposit (facies C). In the glacier-distal part of the outcrop lies a more-deformed unit of lodgment till and glaciofluvial gravel and sand (facies A), with inclusions of reworked peat clasts that include twigs. Three samples of these twigs range in age between 11,450 ± 70 and 11,550 ± 55 ^{14}C yrs BP (13,310 ± 70 to 13,400 ± 70 cal yrs BP). Two tills compose the main body of this stacked moraine ridge, a lower lodgment (facies D) and an upper largely glaciofluvial deformed till unit (facies D_1). After glacier recession, slope instability generated slumps on both sides of the moraine ridge (facies E).

At Site 4 in Fig. 9, numerous peat clasts have been reworked as inclusions into the basal deformation till (facies A) of the 7th recessional moraine ridge of the PB2 series (counting downhill from the outermost PB2 moraine). The deformation till also includes a glaciofluvial inclusion covered by peat. The reworked peat clasts and the larger glaciofluvial inclusion afford numerous radiocarbon ages between 13,300 ± 50 and 12,750 ± 50 ^{14}C yrs BP (16,310 ± 300 and 15,150 ± 190 cal yrs BP). Just as in the other cases, this ridge consists of an accumulation of glaciofluvial sediments (facies C), lodgment till (facies D and D_1), and flow till (facies B).

4.2. Minimum-limiting radiocarbon ages of the Puerto Bandera moraines

Peat bogs and ponds generated in spillways and furrows on top of and inboard of PB moraines were cored for samples that would

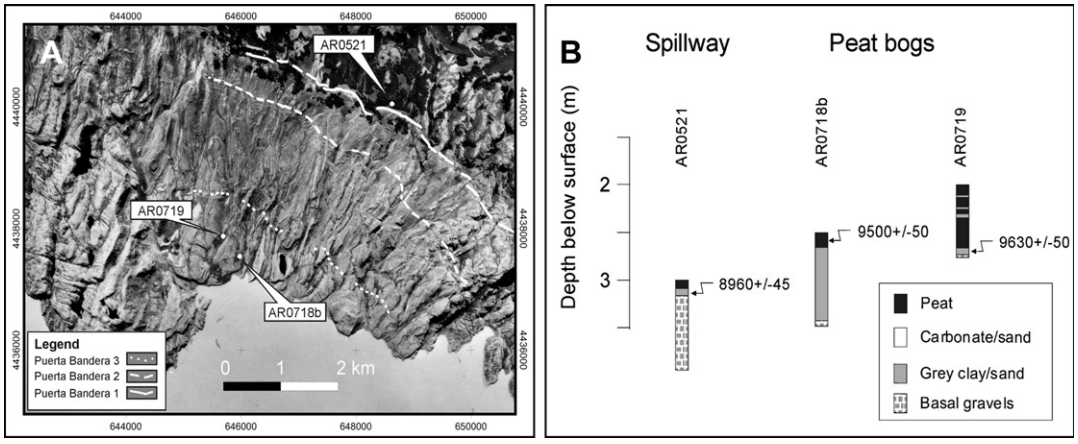

Fig. 10. Vertical air photograph of Bahía del Quemado showing (A) the sample locations and (B) the corresponding lower core sections. The insert shows the legend for all the following descriptions of core sections. White, long segmented, short segmented, and dotted lines indicate PB1, PB2, and PB3 moraines, respectively.

Table 1
Radiocarbon dates of samples collected near Bahía del Quemado. See Fig. 10 for sample locations.

Core	Depth (cm)	Sample description	^{14}C Lab #	^{14}C age	±1σ	Cal yrs	±1σ	Age significance
AR0521	312–313	Twigs	OS-51478	8960	45	10,090	100	Peat grew in spillway, minimum-limiting age for recession from the PB1 moraine
AR0718	260	Twigs	OS-63267	9500	50	10,840	140	Peat bog development, minimum-limiting age for recession from the PB3 moraine
AR0719	272	Wood	OS-63272	9630	50	10,980	120	

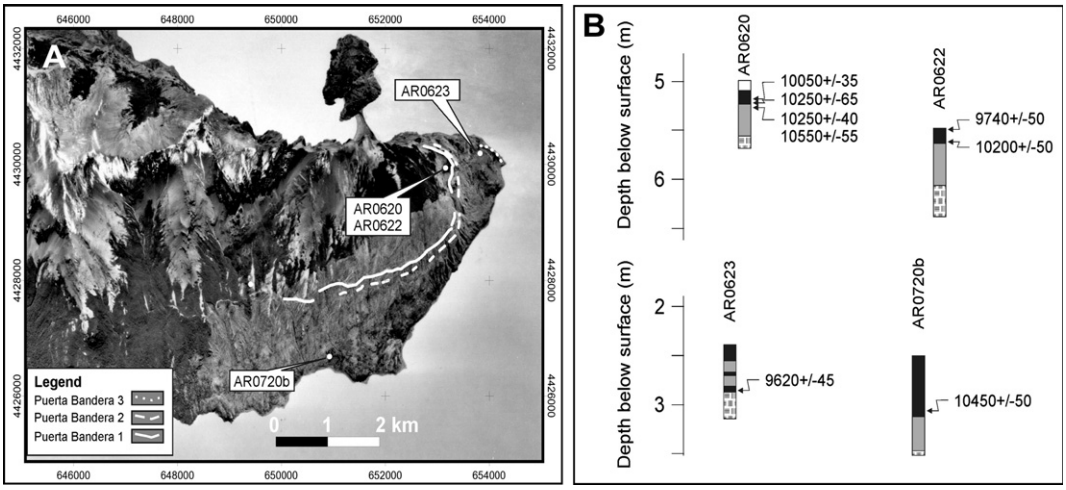

Fig. 11. Vertical air photograph showing (A) sample sites for minimum-limiting ages for glacier recession from Península Avellaneda and (B) lower core sections with dated organic horizons. White, long segmented, short segmented, and dotted lines indicate PB1, PB2, and PB3 moraines, respectively.

provide minimum-limiting radiocarbon ages of ice recession in sectors 1 to 4 (Figs. 1 and 2). Three additional bogs (sectors 5 to 7) and one outcrop (sector 8), all located deep within the western branches of Lago Argentino, were also sampled to determine the timing and magnitude of glacier recession. Herein we describe the samples and discuss the significance of the resulting ages for each sector. Also included are aerial photographs with the location of the sample sites, sketches with the simplified stratigraphy, and tables with the radiocarbon dates.

4.2.1. Sector 1: Bahía del Quemado (Fig. 1)

Two peat bogs were cored at Bahía del Quemado on the ice-proximal side of the PB3 moraine (AR0719 and AR0718b, Fig. 10A). Twigs and pieces of wood were obtained from the base of the 3.6-to-2.8-m-deep peat bogs. The spillway, which drained the outer side of the PB1 moraine when the glacier stood at the proximal side of the moraine, was also sampled for twigs and other organic matter at the base of a 3-m-deep peat layer (AR0521, Fig. 10A).

The resulting ages (Fig. 10B and Table 1) demonstrate that the Brazo Norte glacier retreated from the northeast valley slope alongside Bahía del Quemado prior to 9630 ± 50 ^{14}C yrs BP (10,980 ± 120 cal yrs BP).

4.2.2. Sector 2: Península Avellaneda (Fig. 1)

At Península Avellaneda we cored a hanging peat bog (455 m a.s.l.), located in a furrow between the PB1 and PB2 moraines. The 6.5-m-deep bog (AR0620 and AR0622, Fig. 11A) provided basal peat that included pieces of wood, twigs, and sedge. Two additional peat bogs located close to the present-day lake level (185 m a.s.l.), outboard of PB3 moraine ridges (AR0720b and AR0623, Fig. 11A), were cored to a depth of 4.5 m.

The ages obtained in this sector indicate that the glacier receded from the PB1 moraine prior to 10,550 ± 55 ^{14}C yrs BP (12,490 ± 80 cal yrs BP). Recession from the PB2 moraine occurred more than 10,450 ± 50 ^{14}C yrs BP (12,350 ± 120 cal yrs BP) (Fig. 11B and Table 2).

4.2.3. Sector 3: Brazo Rico glacial-lake spillways (Fig. 1)

At the key site of the Brazo Rico glacial-lake spillways, Mercer (1968) obtained a minimum-limiting age of 10,000 ± 140 ^{14}C yrs BP for glacier withdrawal from the PB moraines. An older minimum-limiting age of 10,390 ± 470 ^{14}C yrs BP, also obtained by Mercer, was published later by Strelin and Malagnino (2000).

Mercer (1968) noted that during glacier recession the former glacier-dammed lake in Brazo Rico was drained by what is here called Spillway M (Fig. 12A), located immediately south of Cerro Frías. This spillway was active until the PB glacier lobe receded to the southwestern tip of Península Magallanes (Figs. 2 and 12A). When the glacier recession reached the position of the present-day front of Perito Moreno Glacier, the drainage of Brazo Rico switched to Canal de los Témpanos, as is the case today. The result of this switch is that Spillway M became inactive and plant colonization was initiated on its floor. The lowest and hence oldest organic material on the floor of Spillway M afforded Mercer (1968) and our samples for minimum-limiting radiocarbon ages for at least 30 km of glacier recession from the PB frontal moraines to the present-day terminus of Perito Moreno Glacier in Canal de los Témpanos.

We also sampled an older spillway called Spillway O (Fig. 12A), which incises only the PB1 moraine. This spillway was active during glacier recession from the PB1 moraine position, until it was blocked by deposition of the PB2 moraine. After that blockage occurred, Spillway M was formed and remained active as the

Table 2
Radiocarbon dates of samples collected on Península Avellaneda. See Fig. 11 for sample locations.

Core	Depth (cm)	Sample description	^{14}C Lab #	^{14}C age	±1σ	Cal yrs	±1σ	Age significance
AR0620	530–531	Wood fragments	OS-58278	10,050	35	11,560	110	Peat bog development, minimum-limiting age of PB1 moraine
AR0620	532–533	Twigs	OS-58495	10,250	65	12,000	150	
AR0620	536–537	Twigs	OS-64829	10,250	40	11,990	90	
AR0620	537–538	Organic sediment	OS-58557	10,550	55	12,490	80	
AR0622	551	Wood fragments	OS-64992	9740	50	11,160	80	
AR0622	561–562	Bulk peat	OS-64972	10,200	50	11,900	100	
AR0623	286–287	Sedge fragments	OS-64963	9620	45	10,970	120	Peat bog development, minimum-limiting age of PB2 moraine
AR0720b	308	Sedge fragments	OS-65010	10,450	50	12,350	120	

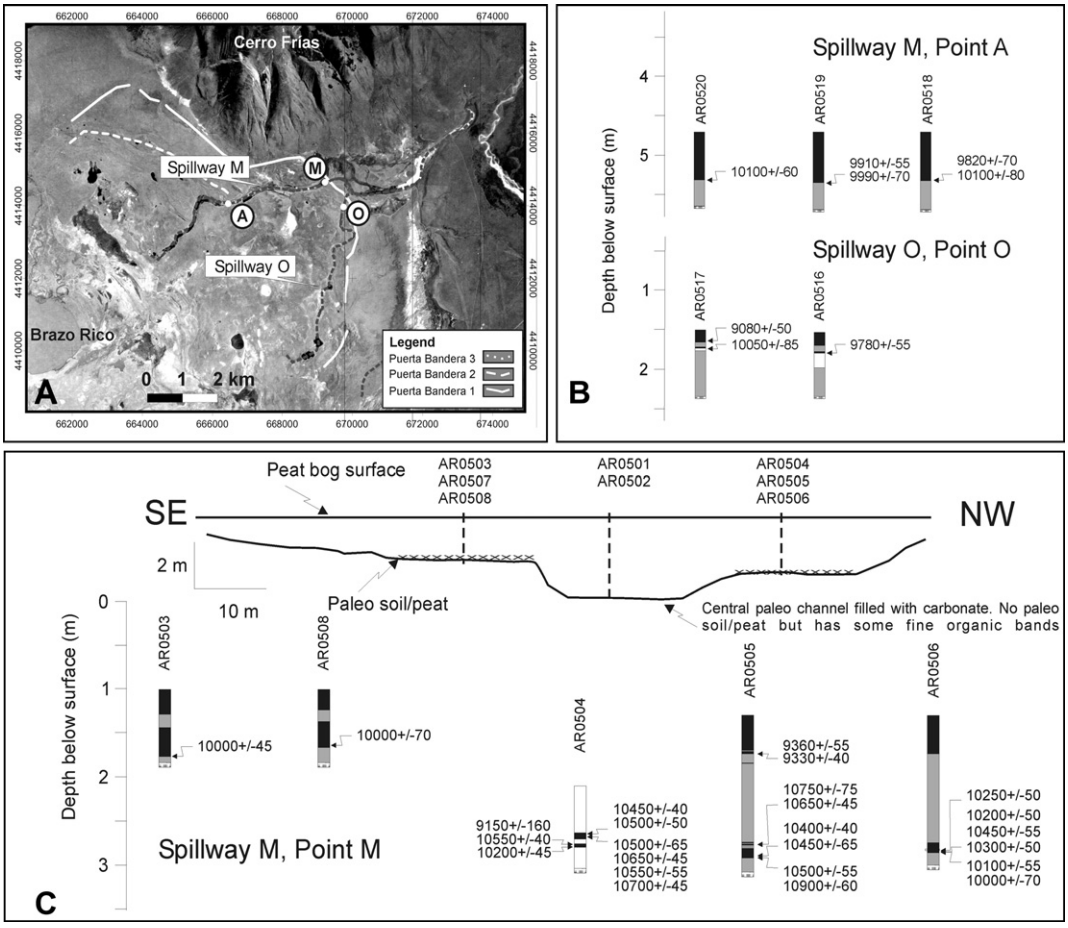

Fig. 12. (A) Vertical air photograph showing the two spillways (M and O) and sample sites (localities A, M, and O) east of Brazo Rico. (B) Basal core sections from two new sites, localities A and O. (C) Section of Spillway M and basal peat core sections at locality M, near the site cored by Mercer (1968). White, long segmented, short segmented, and dotted lines indicate PB1, PB2, and PB3 moraines, respectively.

glacier pulled back from the PB2 and PB3 moraines and receded to the present-day position of Perito Moreno Glacier, at which time the lake in Brazo Rico was able to drain into Lago Argentino through Canal de los Témpanos.

We cored Spillway M at two different places, one at Mercer (1968) site (locality M in Fig. 12) and the other at locality A in Fig. 12A, affording basal peat samples from a depth of 2–5.5 m below the surface. We also cored Spillway O for basal peat (Fig. 12A), but obtained no older minimum age than that assayed from the younger spillway. The dated material in the spillways consists of plant stems, plant fragments, sedge macrofossils, wood fragments, bulk organic sediment, and Carex seeds. Some samples from Spillway M were enclosed in marl sediment considered to be organically precipitated carbonates and have been excluded from chronology development (Fig. 12C and Table 3 footnote).

The oldest minimum-limiting age that we obtained for Spillway M was 10,900 ± 60 ^{14}C yrs (12,780 ± 90 cal yrs BP) derived from bulk organic sand, but the most reliable samples, those containing terrestrial macrofossils including wood, twigs, and moss fragments (Table 3 footnote), gave minimum-limiting ages as old as 10,750 ± 75 (12,660 ± 70 cal yrs BP).

4.2.4. Sector 4: Bahía Catalana (Fig. 1)

Mercer (1968) proposed the existence of a spillway at Bahía Catalana (Figs. 2 and 13A), only 1 km from the present front of Perito Moreno Glacier. He estimated that the highest point of this spillway was 5 m below that of Spillway M (Figs. 2 and 12A). Mercer (1968) considered that the Bahía Catalana "spillway" became active when the former Perito Moreno Glacier receded behind Bahía Catalana. We measured the thresholds of Spillway M and Bahía Catalana using a topographic differential GPS system. According to our measurements, the Bahía Catalana threshold is 224 m and the Spillway M threshold is 205 m above mean sea level (with reference to geoid EGM96). Spillway M therefore controlled the level of Brazo Rico until it was connected with Lago Argentino through Canal de los Témpanos. According to our interpretation, Bahía Catalana was, during its last stage, a melt water channel nourished directly by glacier ice rather than spillover from the lake. This melt channel became inactive when the glacier front receded inboard of Bahía Catalana. Such recession must have occurred shortly before Brazo Rico was connected to Lago Argentino, diverting the lake drainage from Spillway M into Canal de los Témpanos.

A 250-m-long and 40-m-wide peat bog occupies an upper depression in the old melt water channel located in the gap between Bahía Catalana and Canal de los Témpanos (Fig. 13A). Mercer and Ager (1983) provided a minimum age of 9510 ± 210 ^{14}C yrs BP for plant colonization of this bog. We cored the same peat bog at three different places, obtaining basal organic sediments (including seeds) from an isolated peat layer at 3.4–3.6 m depth. An age of 10,400 ± 50 ^{14}C yrs BP (12,280 ± 110 cal yrs BP) was obtained from one of these samples (Fig. 13B and Table 4). The deepest core reaches gravel at 6.8 m depth after penetrating about 3 m of gray laminated clay.

Table 3
Radiocarbon dates from different Brazo Rico spillways sites: spillway A, spillway M, and spillway O. For sample locations see Fig. 12.

Core	Depth (cm)	Sample description	^{14}C Lab #	^{14}C age	±1σ	Cal yrs	±1σ	Age significance
Spillway M, site A								
AR0518	530–531	Wood	OS-51568	9820	70	11,250	90	Minimum age of spillway abandonment
AR0518	530–531	*Carex* seeds	OS-51582	10,100	80	11,680	190	
AR0519	532–533	Wood	OS51566	9910	55	11,350	100	
AR0519	532–533	*Carex* seeds	OS-51570	9990	70	11,490	150	
AR0520	529–530	Plant stems	OS-53251	10,100	60	11,690	160	
Spillway M, site M								
AR0503	176–177	Organic sediment*	OS-52108	10,000	45	11480	120	Minimum age of spillway abandonment
AR0504	264–266	Plant fragments*	OS-64830	10,450	40	12,360	120	
AR0504	264–266	Plant fragments*	OS-64831	10,500	50	12,450	100	
AR0504	266–268	Plant stems*	OS-51564	10,500	65	12,420	120	
AR0504	266–268	Plant fragments*	OS-64839	10,650	45	12,600	40	
AR0504	266–268	Plant fragments*	OS-64840	10,550	55	12490	80	
AR0504	266–268	Plant fragments*	OS-64841	10,700	45	12,630	40	
AR0504	278–279	Plant stems*	OS-53565	9150	160	10,340	230	
AR0504	279–281	Organic fine sand*	OS-64983	10,550	40	12,510	60	
AR0504	281–283	Plant fragments*	OS-64825	10,200	45	11,900	90	
AR0505	174–175	Bark-wood fragments	OS-64842	9330	40	10,540	60	Peat development
AR0505	174–175	Bark-wood fragments	OS-64552	9360	55	10,580	80	
AR0505	277–278	Plant fragments*	OS-64971	10,650	45	12,600	40	Minimum age of spillway abandonment
AR0505	277–278	Wood fragments	OS-64553	10,750	75	12,660	70	
AR0505	289–290	Bryophyte plant fragments	OS-64967	10,450	65	12,340	130	
AR0505	289–290	Bryophyte plant fragments	OS-64970	10,400	40	12,270	100	
AR0505	290–291	Sedge macrofossils*	OS-51727	10,500	55	12,440	110	
AR0505	290–291	Organic fine sand*	OS-64962	10,900	60	12,780	90	
AR0506	283–284	Sedge fragments*	OS-64526	10,250	50	11,990	110	
AR0506	284–285	Bark-wood fragments	OS-64525	10,450	55	12,350	130	
AR0506	284–285	Bark-wood fragments	OS-64551	10,300	50	12,120	130	
AR0506	284–285	Wood fragments	OS-64550	10,200	50	11,900	100	
AR0506	285–286	Plant stems*	OS-51728	10,100	55	11,690	160	
AR0506	285–286	Organic sediment*	OS-64668	10,000	70	11,510	150	
AR0508	165–166	Wood	OS-51565	10,000	70	11,510	150	
Spillway O, site O								
AR0516	178–179	Organic sediment	OS-51981	9780	55	11,200	60	Minimum age of spillway abandonment
AR0517	174–175	Organic sediment	OS-51729	10,050	45	11,570	130	
AR0517	165–166	Organic sediment	OS-51726	9080	50	10,250	50	Peat development

Notes: Cores from Spillway M, site M (AR0504, AR0505 and AR0506) contained carbonaceous marl-like deposits at depths close to or around samples selected for AMS dating. As a precaution against the possible contamination of some of these samples from hard-water effects, AMS samples originating from aquatic plant remains or bulk sediment that might have been influenced by organically precipitated carbonate have been removed from consideration for chronology development. These are indicated by asterisks (*) in the sample description column. Samples originating from terrestrial origin including wood, twigs, and moss fragments are considered to provide robust age estimates at this site.

The development of the peat bog would only have been possible once glacier recession reached inland of Bahía Catalana and melt waters ceased to drain through the channel that connected Bahía Catalana with Canal de los Témpanos. It follows that cessation of melt water flow must have occurred prior to 10,400 ± 50 ^{14}C yrs BP (12,280 ± 110 cal yrs BP), the age of the oldest basal peat in the channel (Table 4).

4.2.5. Sector 6: Herminita moraines (Fig. 1)

About five moraine ridges making up a moraine complex were mapped on the southern tip of Peninsula Herminita. Four 2-to-6-m-deep peat bogs were cored inboard of this interlobate Herminita moraine complex (Malagnino and Strelin, 1992), providing basal peat samples for radiocarbon dating (Fig. 14A and B).

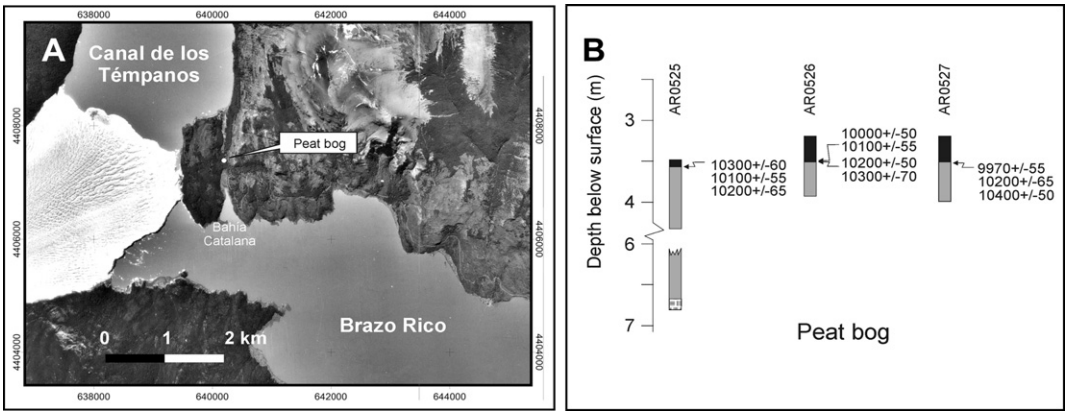

Fig. 13. (A) Vertical air photograph showing sample sites in the Bahía Catalana melt water channel presently occupied by a peat bog. (B) Basal core sections.

Table 4
Radiocarbon dates of basal organic material from Bahía Catalana peat bog. See Fig. 13 for locations of the cores from which the samples were collected.

Core	Depth (cm)	Sample description	^{14}C Lab #	^{14}C age	±1σ	Cal yrs	±1σ	Age significance
AR0525	358–359	Organic sediment	OS-51734	10,300	60	12,120	140	Minimum age of spillway abandonment
AR0525	358–359	Organic sediment	OS-64542	10,100	55	11,690	160	
AR0525	358–359	Organic sediment	OS-64539	10,200	65	11,890	140	
AR0526	346–347	Organic sediment	OS-64543	10,000	50	11,490	120	
AR0526	346–347	Organic sediment	OS-64544	10,100	55	11,690	160	
AR0526	347–348	Plant fragments	OS-51735	10,200	50	11,900	100	
AR0526	347–348	Organic sediment	OS-51956	10,300	70	12,120	160	
AR0527	350–351	Organic sediment	OS-64540	9970	55	11,440	120	
AR0527	350–351	Organic sediment	OS-64529	10,200	65	11,890	140	
AR0527	350–351	Organic sediment	OS-51736	10,400	50	12,280	110	

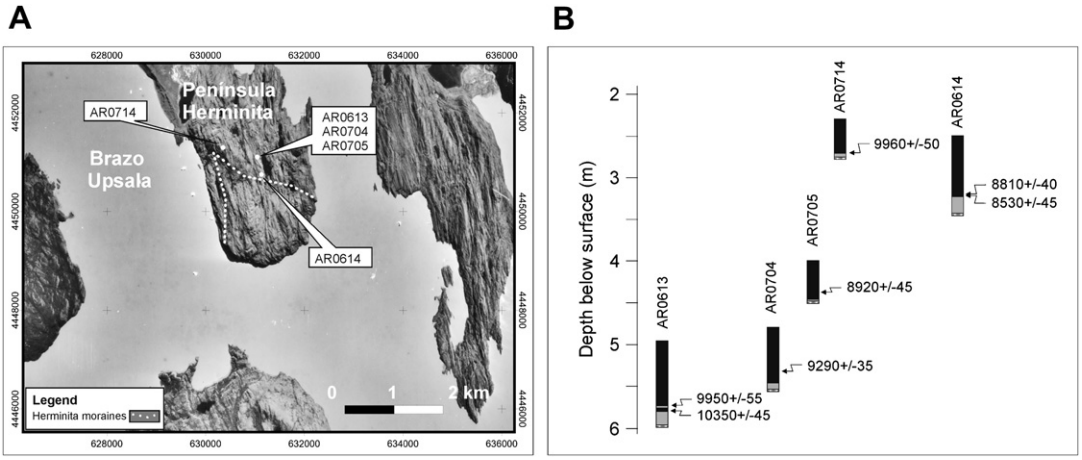

Fig. 14. (A) Vertical air photograph showing the location of the peat bog sample sites just inboard of the Herminita moraines (dotted white line). (B) Dated basal core sections.

Table 5
Radiocarbon dates of basal material from peat bogs inboard of the Herminita moraines. See Fig. 14 for location of the cores from which the samples were collected.

Core	Depth (cm)	Sample description	^{14}C Lab #	^{14}C age	±1σ	Cal yrs	±1σ	Age significance
AR0613	571–572	Organic sediment	OS-64990	9950	55	11,410	120	Peat bog development, minimum
AR0613	575–576	Organic sediment	OS-58594	10,350	45	12,220	110	age of Herminita moraines
AR0704	535	Plant fragments	OS-65004	9290	35	10,480	60	
AR0705	439	Plant fragments	OS-65005	8920	45	10,050	90	
AR0714	270	Organic sediment	OS-65007	9960	50	11,420	120	
AR0614	318–319	Bulk peat	OS-64991	8810	40	9870	120	
AR0614	321–322	Plant fragments	OS-58493	8530	45	9510	20	

The oldest date is 10,350 ± 45 ^{14}C yrs BP (12,220 ± 110 cal yrs BP), affording a minimum age for the plant colonization inboard of the Herminita moraines (Table 5). Thus the Herminita moraines, as well as the PB moraines, are late-glacial in age.

4.2.6. Sectors 5, 7, and 8: glacier recession (Fig. 1)

The importance of these sectors is that they show the magnitude of ice recession into the Lago Argentino tributary valleys following deposition of the Puerto Bandera moraines.

Near Lago Frías, Brazo Sur of Lago Argentino (Sector 5 in Fig. 1), basal silty peat was obtained from a 2.58-m-deep bog located immediately outboard of the outermost Neoglacial moraine. The results show that the glacier front had retreated behind this position prior to 10,400 ± 40 ^{14}C yrs BP (12,270 ± 100 cal yrs BP) (Table 6).

Two terminal moraines (Pearson 1 and Pearson 2; Mercer, 1965) are the most conspicuous landforms immediately south of Lago Pearson (Anita) (Sector 7 in Fig. 1). They were deposited when the

Table 6
Lago Frías, Lago Pearson (Anita), and Agassiz Este Valley radiocarbon samples and ages.

Sample and sample sector	Depth (cm)	Sample description	^{14}C Lab #	^{14}C age	±1σ	Cal yrs	±1σ	Age significance
AR0723	258	Organic sediment	OS-64999	10,400	40	12,270	100	Basal peat immediately outboard of the Neoglacial moraines
Lago Frías								
AR0608	223	Sedge fragments	OS-64966	9040	45	10,210	50	Basal peat immediately outboard of Neoglacial moraines
Lago Pearson (Anita)								
LA0704		Wood fragment	OS-63465	8160	60	9130	90	Wood in diamicton below glacigenic units
Agassiz Este								
AR0616 Agassiz Este		Wood fragment	OS-58599	8290	40	9300	80	Wood in diamicton below glacigenic units
AR0717 Agassiz Este		Wood fragment	OS-58601	8210	35	9170	70	Wood in diamicton below glacigenic units

bedrock ridge that separates Upsala Glacier from Lago Pearson (Anita) was repeatedly overridden by ice during the Holocene, generating two glacier lobes and related moraine deposits.

Basal peat, cored at a depth of 2.23 m in front of the Neoglacial Pearson 1 moraine south of Lago Pearson (Anita), Sector 7 (Fig. 1), indicates extensive glacier withdrawal prior to 9040 ± 45 ^{14}C yrs BP (10,210 ± 50 cal yrs BP) (Table 6). Mercer and Ager (1983) provided a similar date of 9010 ± 215 ^{14}C yrs BP for glacier shrinkage to the Neoglacial position in this sector immediately east of the Southern Patagonian Icefield.

Close to the present-day Agassiz Este Glacier front (Sector 8 in Fig. 1) several small pieces of wood were collected from the base of an exposure that was cut deep inside a gully. The wood fragments were incorporated into a diamicton, which does not appear to be a till, covered by middle to late Holocene glaciogenic deposits. The wood fragments in the diamicton yielded radiocarbon ages of 8160 ± 60 to 8290 ± 40 ^{14}C yrs BP (9130 ± 90 to 9300 ± 80 cal yrs BP) (Table 6). This diamicton crops out at the foot of a scar and was probably generated by mass wasting after the most extensive post-late-glacial deglaciation. The stratigraphy of this sector indicates that before ~9300 cal yrs BP, the glacier receded very close to, or behind, the present glacier front.

5. The late-glacial depositional history of the Puerto Bandera moraines

The depositional history of the PB moraines was reconstructed from the interpretation of the morphostratigraphy and of the dates of radiocarbon samples collected in moraine exposures along the topographic cross section on the northern slope of Bahía del Quemado (Figs. 4–9), and from minimum-limiting ages obtained from abandoned spillways, peat bogs, and outcrops located at, and inboard of, the outer PB moraines (Figs. 10–14 and Tables 1–6). Additional figures were drawn (Figs. 15–17) to improve the understanding of the absolute chronology assigned to the late-glacial landscape evolution of the Lago Argentino basin.

After the LGM, during an important interval that began by at least 13,450 ± 150 ^{14}C yrs BP (16,440 ± 340 cal yrs BP), as indicated by dates of twigs from a lower peat inclusion in the PB deformation till at Site 2 (Fig. 7), the former Lago Argentino glacier receded from Bahía del Quemado (Figs. 4 and 15A, and 16A). Peat bogs then grew on the newly deglaciated valley slope adjacent to this bay. Additional dates of the uppermost peat in this same inclusion, as well as from the peat clasts incorporated in basal deformation till at Site 3 (Fig. 8) and Site 4 (Fig. 9), show that the ice terminus remained inboard of subsequent PB moraine positions for at least 2000 years (Fig. 17A and B).

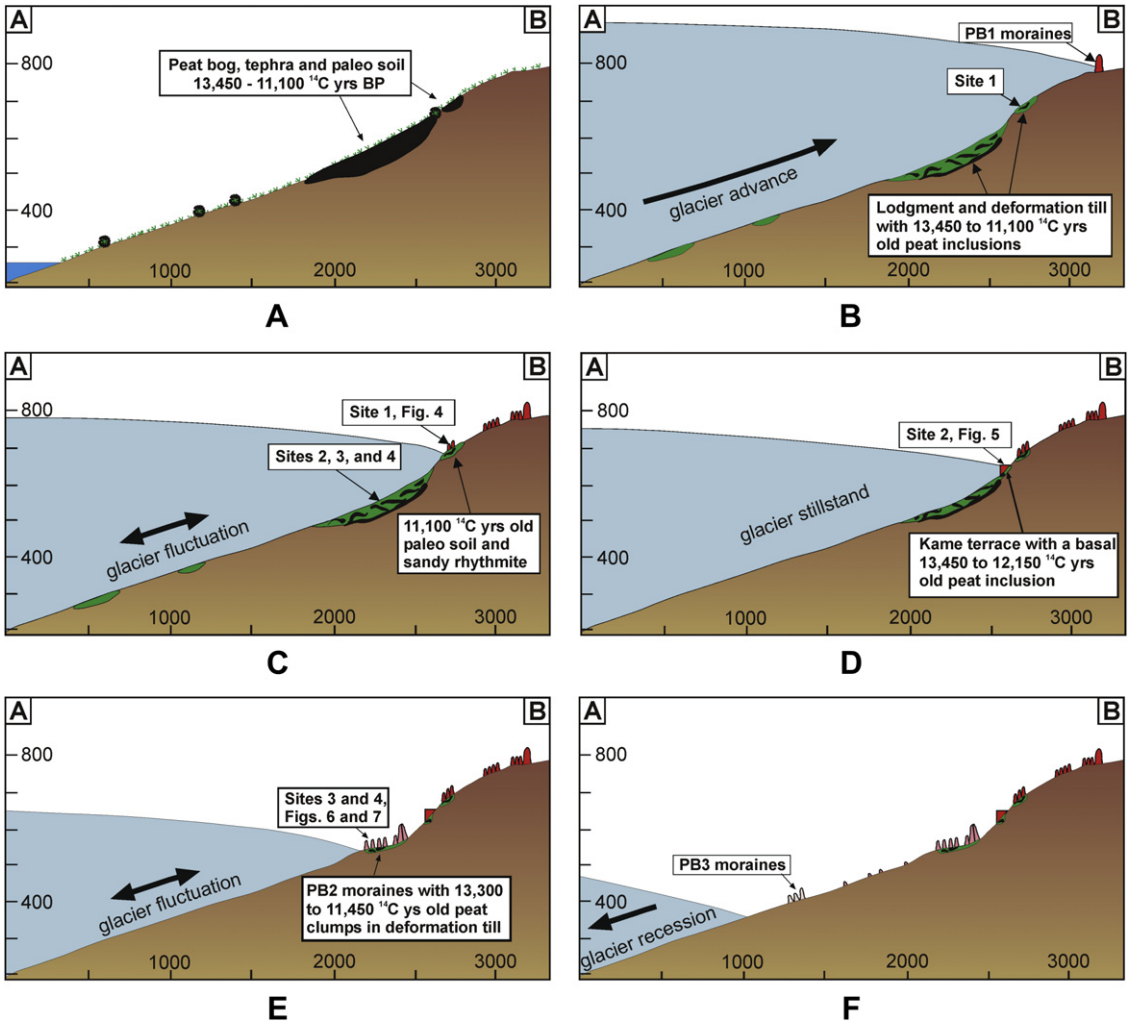

Fig. 15. (A) Post-LGM glacial recession, (B) PB1 late-glacial advance, (C) piling up of PB1 recessional moraine ridges, (D) PB1 kame terrace formation, (E) PB2 moraine formation, (F) PB3 moraine formation and recession. For location of this cross section see Fig. 4A and B. Recessional moraines were generated during glacier fluctuations.

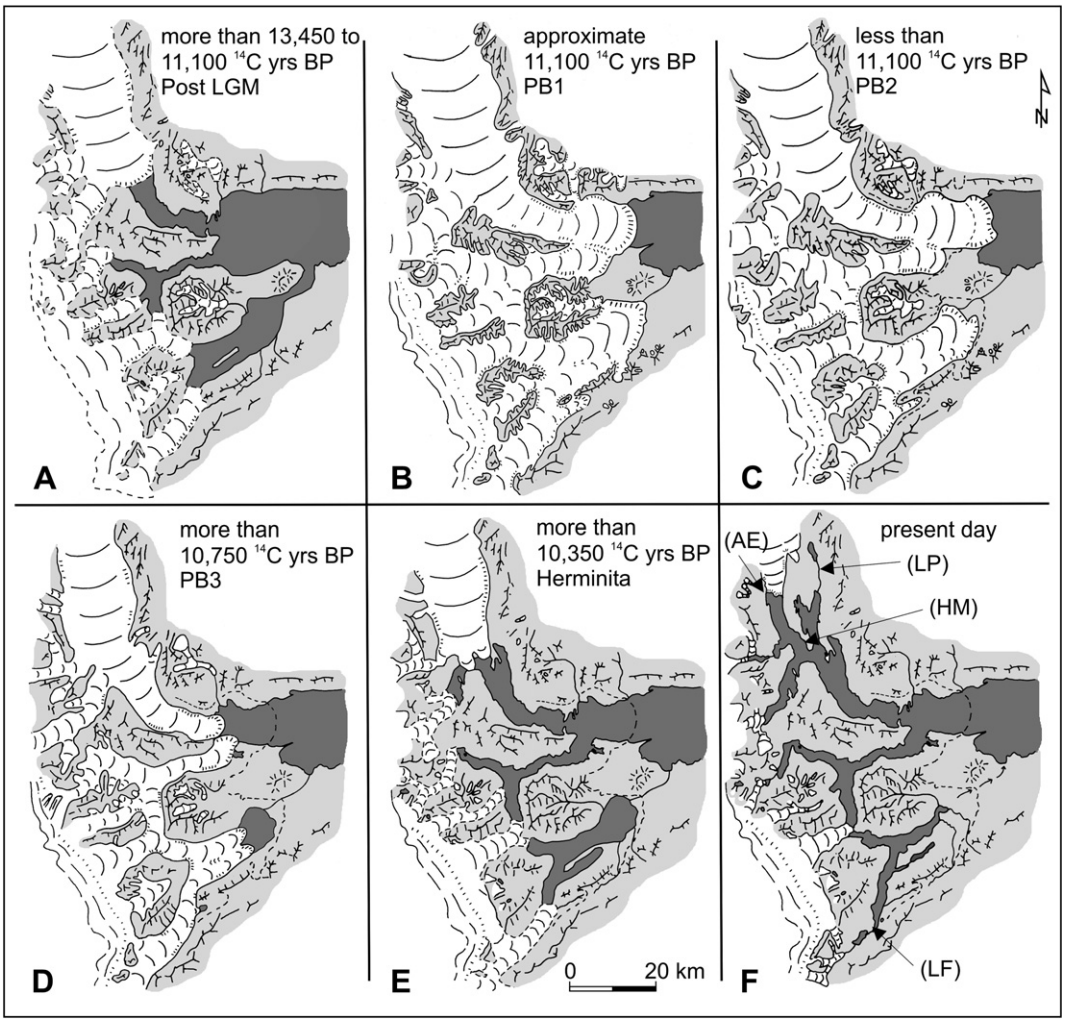

Fig. 16. Reconstruction of glacier fluctuations during the late-glacial in Lago Argentino. (A) Post-LGM glacier recession (see also Fig. 15A), (B) PB1 advance (see also Fig. 15B), (C) PB2 advance, (D) PB3, (E) Herminita advance, (F) present situation. AE: Agassiz Este valley. LP: Lago Pearson (Anita). HM: Herminita moraines. LF: Lago Frías.

The simplest interpretation of the stratigraphy described above, along with radiocarbon dates is that, after the glacier recession (post-LGM), the former Lago Argentino glacier underwent a major advance that reached the western part of the main body of Lago Argentino (Figs. 15B and 16B) and overrode the northern slope of Bahía del Quemado, about 25 km behind the calving front farther east in Lago Argentino. Basal deformation till (colored green with black spots in Fig. 15B) generated during this major advance, along with inclusions composed of glaciofluvial deposits, peat clasts, relic soil, and fallout tephras, were transported in the glacier sole and deposited at the base of the moraine ridges exposed in the sections from Site 1 to Site 4 (Figs. 6–9). The advancing Lago Argentino glacier overrode Site 1 (Figs. 15B and 16B) at or very shortly after 11,100 ± 60 ^{14}C yrs BP (12,990 ± 80 cal yrs BP, Fig. 17A and B) and achieved its maximum lateral expansion when it deposited the PB1 outer moraine ridge at 740 m (a.s.l.).

Alternative but less likely explanations of the data are possible. For example, one could postulate that the maximum-limiting age afforded by the peat incorporated into the deformation till of Site 3 (Facies A in Fig. 8) and dated to 11,450 ± 70 ^{14}C yrs ago (13,310 ± 70 cal yrs BP) and the deformation till at Site 1 (Facies A in Fig. 6), including the tephra and soil layer, represent an ice-marginal fluctuation during general recession from the outermost PB1 moraine. In this case the date of 11,100 ± 60 ^{14}C yrs BP (12,990 ± 80 cal yrs BP) would be a minimum-limiting age for general recession from the outermost PB1 moraine. We consider this second interpretation to be improbable because the long time required for the soil formation and plant colonization in Site 1 is incompatible with a short-lived fluctuation during overall glacier recession. In addition, the presence of a basal deformation till (Facies A) as the lowest unit in all four exposures (Sites 1 to 4, Figs. 6–9) implies a major glacier advance across all the stratigraphic sections to the outer PB1 moraine.

Overall recession from the outer PB1 moraine was marked by a series of short ice-marginal oscillations of steadily decreasing extent, which resulted in recessional moraine ridges of PB1, composed of lodgment and flow tills deposited on top of the basal deformation till in Site 1 (Figs. 6 and 15C). A short stabilization of the ice margin during PB1 was recognized by the accumulation of a large amount of ice-contact outwash sediments in a kame terrace at Site 2 (Figs. 7 and 15D). Only a minor reworked moraine ridge remains on top of this terrace. A large peat and glaciofluvial inclusion occurs at the base of this outcrop (Fig. 7).

An important glacier readvance deposited the main PB2 moraine that probably buries the youngest PB1 recessional moraines. Only on the margins of the calving Brazo Norte glacier lobe did the PB2 moraines override the outer PB1 moraines (Figs. 2 and 16C).

In Bahía del Quemado, the main PB2 glacier advance was followed by the deposition of a series of smaller recessional ridges at Sites 3

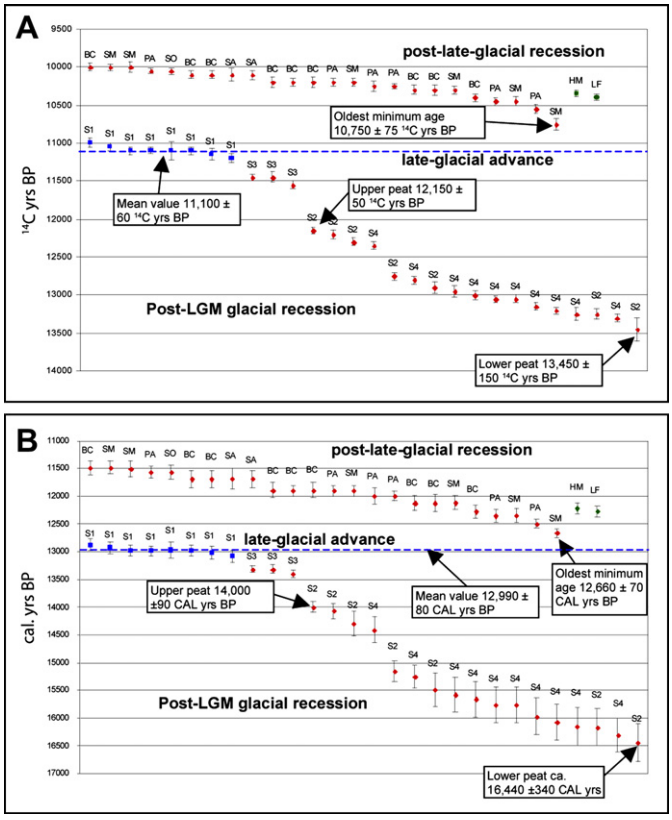

Fig. 17. Radiocarbon (A) and calibrated (B) (OxCal 4.1.5 software, Bronk Ramsay, 2010 and the IntCal09 curve of Reimer et al., 2009) ages for samples associated with the PB moraines, Lago Argentino. Samples S1 to S4 correspond to Sites 1 to Site 4 from Bahía del Quemado (Figs. 6–9). Minimum-limiting ages for pre-late-glacial and post-late-glacial recession are indicated in red dots. "Lower peat" and "upper peat" labels indicate the extreme (maximum and minimum) ages obtained from the two peat layers located within the large inclusion of Site 2 (Fig. 7). Close maximum-limiting ages ($n = 8$) for the accumulation of PB1 moraines are indicated in blue dots; the mean age of these samples is 11,100 ± 60 ^{14}C yrs BP (12,990 ± 80 cal yrs BP) and is plotted in a blue dashed line. Peninsula Avellaneda (PA), Brazo Rico spillways (SA, SM, and SO), and Bahía Catalana (BC) samples, plotted as red dots, correspond to minimum-limiting ages of glacier recession from the PB moraine positions. Herminita moraines (HM) and Lago Frías (LF) samples, plotted as green dots, indicate the minimum-limiting ages for post-PB glacier recession far up valley.

and 4 (Fig. 15E). The 6th and 7th PB2 moraine ridges (counting downslope) were accumulated, respectively, at 570 and 540 m (a.s.l.). As is shown in Fig. 15E, deformation till, with inclusions of reworked peat clasts (colored green with black spots), also occurs at the base of stratigraphic sections exposed in these recessional moraines. The Lago Argentino glacier then continued to retreat, with only short interruptions during which three well-defined PB3 moraine ridges were deposited close to 390 m a.s.l (Figs. 15F and 16D).

After glacier recession from the PB moraines, the inland branches of Lago Argentino became vegetated, and bogs accumulated on the newly deglaciated terrain. Radiocarbon samples collected from the basal organic material in such bogs afforded the oldest minimum-limiting age of 10,750 ± 75 ^{14}C yrs BP (12,660 ± 70 cal yrs BP, Fig. 17B) for the abandonment of Spillway M in Brazo Rico (SM in Fig. 17A and B). An additional minimum-limiting age of 10,550 ± 55 ^{14}C yrs BP (12,490 ± 80 cal yrs BP) was obtained for the plant colonization behind PB1 moraines in Península Avellaneda (PA in Fig. 17A and B), as well as 10,400 ± 50 ^{14}C yrs BP (12,280 ± 110 cal yrs BP) for the abandonment of the melt water channel in Bahía Catalana (BC in Fig. 17A and B). A minor glacier advance or still-stand deposited Herminita moraines 20-km south of the present glacier front (Fig. 16E and F). Dates of 10,350 ± 45 ^{14}C yrs BP (12,220 ± 110 cal yrs BP) and 10,400 ± 40 ^{14}C yrs BP (12,270 ± 100 cal yrs BP) were acquired from basal peat samples collected immediately inboard of the Herminita moraines (HM in Figs. 16F, 17A and 17B) and immediately outboard of Lago Frías Holocene moraine (LF in Figs. 16F, 17A and 17B), respectively. These sets of radiocarbon dates (Fig. 17A and B) indicate rapid and extensive glacier recession after construction of the PB moraines. Overall recession reached close the present-day glacier front near Lago Pearson (Anita) (Sector 7 in Fig. 1 and LP in Fig. 16F) and in Agassiz Este Valley (Sector 8 in Fig. 1 and AE in Fig. 16F) by 9040 ± 45 and 8290 ± 40 ^{14}C yrs BP (10,210 ± 50 and 9300 ± 80 cal yrs BP), respectively.

6. Discussion

We now attempt to place the PB moraines in the context of Southern Hemisphere climate change. We start by comparing the chronology and interpretation of the PB moraines with similar moraines in the Southern Alps of New Zealand. We then compare the PB moraine chronology with the isotopic record from a marine-sediment core off of the Chilean Lake District and also with the isotopic signature from the EPICA Dome C ice core from the East Antarctic plateau.

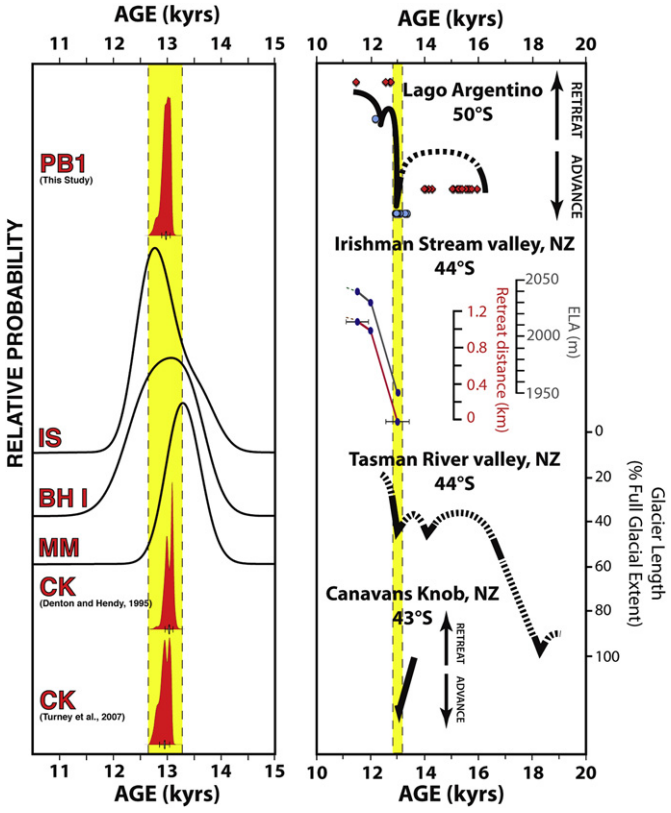

Fig. 18. Comparison of glacier records from Lago Argentino and South Island, New Zealand. Left panel: probability distribution plots dating moraine construction at Lago Argentino and various New Zealand sites. PB: Puerto Bandera moraine (this study). IS: Irishman Stream valley outer moraine, New Zealand (Kaplan et al., 2010). BH I: Birch Hill outer moraine, New Zealand (Putnam et al., 2010). MM: mid-Macaulay moraine, New Zealand (Putnam et al., 2010). CK: Canavans Knob till (from Denton and Hendy, 1994; Turney et al., 2007). Right Panel: records of glacier behavior over the last glacial termination. Top is our schematic time-distance glacier reconstruction from Lago Argentino. Radiocarbon dates documenting ages of recession are shown as red diamonds, and ages relating to moraine construction at the culmination of a glacier advance are plotted as blue circles. Irishman Stream valley equilibrium-line altitude (ELA) and retreat distance reconstruction is from Kaplan et al. (2010). Tasman River valley glacier-length reconstruction is from Putnam et al. (2010). Schematic glacier reconstruction from Canavans Knob is based on the dates of Denton and Hendy (1994) and Turney et al. (2007).

The glaciers in the Southern Alps of New Zealand experienced similar behavior to that of the Lago Argentino glacier (Fig. 18). Franz Josef Glacier, situated northwest of the main drainage divide (Main Divide) of the Southern Alps, advanced over Canavans Knob toward the Waiho Loop moraine at 13,030 ± 40 yrs ago (Denton and Hendy, 1994) or 12,950 ± 90 yrs ago (Turney et al., 2007). To the south of the Main Divide, a large, former glacier that drained the Aoraki/Mount Cook sector of the Southern Alps advanced to the prominent Birch Hill moraines in the Tasman River valley at 12,970 ± 300 yrs ago, followed immediately by recession (Putnam et al., 2010). In the Macaulay River valley a former glacier advanced to a prominent late-glacial moraine at 13,310 ± 290 yrs ago (Putnam et al., 2010). Finally a former glacier in the Irishman Stream valley in the Ben Ohau Range, an offshoot of the Southern Alps, advanced to a sharply defined late-glacial moraine at 13,000 ± 500 yrs ago and shortly thereafter underwent recession so that by 12,200 ± 400 yrs ago the glacier terminus was situated at the valley head (Kaplan et al., 2010). From this comparison in Fig. 18, we infer that the glacier signature was similar in middle southern latitudes in mountains on both sides of the Pacific Ocean. In both Patagonia and the Southern Alps of New Zealand, glacier advance culminated close to 13,000 yrs ago (within error) and was followed by recession over the next <1000 yrs.

Fig. 19 compares Lago Argentino glacier fluctuations since the LGM with an isotope record from a marine-sediment core taken at ODP Site 1233, a short distance off shore of the southern Chilean Lake District. The planktonic foraminiferal $\delta^{18}O$ (*G. bulloides*) record from ODP Site 1233 illustrates changes in surface mixed layer physical properties, such as temperature and salinity ($\delta^{18}O_{water}$). The deglacial change in $\delta^{18}O$ exceeds 2.5‰, equivalent to a warming of more than 6 °C, once whole-ocean changes in $\delta^{18}O_{water}$ are taken into account. This is identical to the magnitude of the deglacial change inferred from lower resolution alkenone-based SST reconstructions from the same core (Lamy et al., 2007), suggesting that the planktonic $\delta^{18}O$ signal is predominantly temperature driven and that there is little or no glacial-interglacial change in local salinity ($\delta^{18}O_{water}$) (Lamy et al., 2004). Although strongly similar to the alkenone SST reconstruction, the *G. bulloides* $\delta^{18}O$ record is used here due to its higher resolution and because it represents ocean mixed layer conditions (King and Howard, 2005). Also, it is not subject to potential age offsets (with the dated sand fraction proxies), which could affect the fine-scale comparisons (e.g., Mollenhauer et al., 2005; Lamy et al., 2007). The close correspondence with benthonic foraminiferal $\delta^{18}O$ at this site (recording changes in Antarctic Intermediate water property) attests to the regional character of the $\delta^{18}O$ signal, as Antarctic Intermediate Water acquires its properties in the Antarctic Polar Frontal Zone well south of ODP Site 1233 (Talley, 2008).

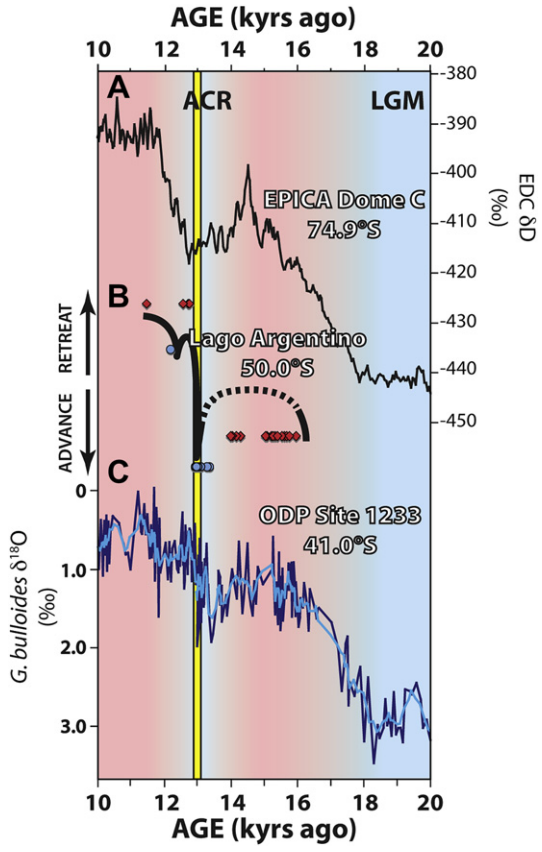

Fig. 19. Deglacial records mentioned in text. Panel A: EPICA Dome C deuterium record, a proxy for Antarctic atmospheric temperature (Lemieux-Dudon et al., 2010). Panel B: schematic diagram depicting the advance of the glacier that produced the Puerto Bandera moraines, placed on the chronology developed from radiocarbon dates presented here. Symbols are described in Fig. 18. Panel C: ODP Site 1233 *G. bulloides* $\delta^{18}O$ record from off shore Chile, reflecting near-surface temperature and salinity changes. Dark blue curve is based on raw data; light blue line is 5-pt running mean.

Fig. 19 also depicts the deuterium record over the last termination from EPICA Dome C, situated at 74.9°S latitude at 3233 m elevation on the East Antarctic plateau (Lemieux-Dudon et al., 2010). This deuterium record is most simply interpreted as a proxy for temperature.

All three curves in Fig. 19 display a common signal of the Antarctic Cold Reversal (ACR) a bit more than halfway through the termination. In all three cases the ACR culminates at 13,000 years ago (within error), followed by rapid warming in the case of ODP 1233 and EPICA Dome C, and by glacier recession in the case of Lago Argentino. Moreover, comparison of Figs. 18 and 19 illustrates that this same ACR signal is also common to the central Southern Alps of New Zealand. Finally, although not depicted in the diagrams, other records of SST near the Subtropical Front (STF), which marks the northern boundary of the Southern Ocean, show a similar reversal of climate during the ACR, followed immediately by warming. These records come from south of Australia at 36°S (Calvo et al., 2007) and in the South Atlantic at 41°S (Barker et al., 2009), and are summarized in Putnam et al. (2010).

We interpret the overall results in Figs. 18 and 19 to reflect a common ACR climate signal that extends in the atmosphere from the top of the Antarctic Ice Sheet to over the Southern Patagonian Icefield in the southern Andes and over the central Southern Alps in New Zealand, as well as in the Southern Ocean as far equatorward as the STF. Thus any explanation must encompass a widespread footprint of the ACR in both the atmosphere and the ocean across at least the southern quarter of the globe. It follows from the chronology in Figs. 18 and 19 that this widespread late-glacial cold reversal is asynchronous with millennial-scale climate changes in the North Atlantic sector of the Northern Hemisphere. The coldest trough of the southern reversal occurred at, or just before, the onset of the cold northern Younger Dryas stadial. Subsequent southern warming and glacier retreat took place during the time of the northern Younger Dryas stadial. A long-standing explanation for such anti-phased behavior is weakened North Atlantic overturning during northern stadials, which resulted in warming of the Southern Hemisphere. In addition such weakened overturning could have led to increased formation of southern deep-water, thereby warming the Southern Ocean.

Another important factor may have contributed to southern warming, augmenting the operation of a bipolar seesaw in the ocean. Lamy et al. (2004, 2007) and Kaiser et al. (2005), consistent with earlier suggestions by Heusser (1989) and Moreno et al.

(1999), argued that the Southern Hemisphere westerlies near southern South America shifted equatorward during the LGM. In addition, a case has been made that during the last termination the westerly wind belt of the Southern Hemisphere shifted poleward during each northern stadial (and equatorward during each northern interstadial) (Anderson et al., 2009; Denton et al., 2010). Such climate-related shifts in the winds would warm/cool the Southern Ocean by regulating a net southward/northward redistribution of heat, accompanied by feedbacks from a contracted/expanded apron of sea ice on the Southern Ocean.

These two processes, which likely were complementary, could have caused the Southern Ocean to expand equatorward and to cool during the northern Bolling/Allerod interstadial, thus producing the widespread southern ACR signal depicted in Figs. 18 and 19. SST in the southeast Pacific Ocean would have been very sensitive to latitudinal shifts of the Southern Hemisphere westerlies (Kaiser et al., 2005). As shown in Fig. 19, the temperature changes of the upper mixed layer of the ocean at ODP Site 1233 correspond closely with fluctuations of the Lago Argentino glacier during late-glacial time. A plausible contribution to such coupling is latitudinal shifts of the westerly wind belt, along with SST, upwind of western South America. Such variations in the temperature of the Southern Ocean could well have provided a changing heat source to stimulate the advance/retreat of the Lago Argentino glacier that occurred during late-glacial time.

Finally, we note that recession of the former Lago Argentino glacier before and after the ACR, documented above, was coeval with the two pulses of increased atmospheric CO_2 registered in the EPICA Dome C ice core from the East Antarctic plateau (Monnin et al., 2001). Such correspondence in timing leaves open the possibility that the warming effect of these increases in atmospheric CO_2 also contributed significantly to recession of the Lago Argentino glacier during the last termination.

Acknowledgements

We are grateful to the Comer Science and Education Foundation (CSEF), Instituto Antártico Argentino (IAA) and Centro de Investigaciones en Ciencias de la Tierra (CICTERRA), Universidad Nacional de Córdoba (UNC), for supporting the research of JS in Patagonia. GHD, AEP, and MJV were supported by the National Oceanic and Atmospheric Administration (NOAA). NOAA also provided funds for radiocarbon dating. In this multidisciplinary expedition several colleagues worked on their own specialties and we are grateful for their kind company and help: Dr Michael Kaplan from Lamont-Doherty Earth Observatory of Columbia University (exposure cosmogenic dating), Dr Randall Keller from Oregon State University (tephrochronology), and Geol. Cesar Toerielli from UNC (dendrochronology). Scott Travis (from CSEF) and the following students from UNC and the University of Maine assisted us during the field work: Lucas Oliva, Nadia Curetti, Juan Pablo Lovecchio, Fernando Calabozo, Juan Presta, Adrián Heredia, Samuel Kelley, Mateo Martini, and Juan Luis Garcia. For logistic support we thank Alejandro Tur, the skipper of Olimpo, our lake transport, and his assistant, Lucas Sobral. Finally we are grateful to the following institutions and people that assisted us during the different field expeditions: Hielo & Aventura (José Pera), Estancia Cristina (Daniel Moreno), and Administración de Parques Nacionales (Guardaparque Fernando Spikermann).

Appendix

Facies description and interpretation.

Geomorphic and stratigraphic evidence was used to reconstruct the glacial valley-side environment of Bahía El Quemado. Five proglacial, subglacial and ice-contact facies were distinguished. The main diagnostic characteristic of each lithofacies was described and the corresponding genetic interpretation was provided.

Facies A

Matrix-to-clast-supported pebbly diamicton that includes deformed sediments of facies B and C. Contacts disturbed and irregular. In places outwash units are associated with peat, tephra, and soil, which appear as reworked inclusions.

Genetic interpretation: glaciofluvial and glaciolacustrine outwash disturbed by an advancing glacier. The ice-marginal fluvial and lacustrine deposits were disturbed (folded and faulted) by debris flows and advancing ice, and sometimes included in or covered by flow and lodgment till (Facies D).

Facies B

Diamictons and inversely graded pebbly-to-silty, diagonally cross-bedded strata, with fine rhythmic laminated sandy-to-clayey distal subfacies. This facies includes some boulders in the upper, proximal diamictons. Lower contacts are sharp and planar, and occur largely on the lee side of the moraine ridges.

Genetic interpretation: glacier readvance that partially ponded the ice-marginal zone; flow tills originated on the sediment-rich sloping glacier surface, entering a shallow, small lake or stream and producing thin turbidites.

Facies C

Gravelly-to-sandy planar/trough cross-bedded sets that grade upward and distally to rhythmically laminated fine sandy-to-clayey deposits. Contacts sharp to transitional, planar to concave.

Genetic interpretation: ice-proximal glaciofluvial and glaciolacustrine.

Facies D

Massive matrix-supported diamicton layers, with abundant striated and faceted boulders and coarse pebbles, embedded in a fine

Table A1
Radiocarbon dates of all samples listed by location.

Location	Core	Depth (cm)	Sample description	^{14}C Lab #	^{14}C age	±1σ	Cal yrs	±1σ	Age significance
Bahía del Quemado	AR0521	312–313	Twigs	OS-51478	8960	45	10,090	100	Peat grew in spillway, minimum-limiting age for recession from the PB1 moraine
	AR0718	260	Twigs	OS-63267	9500	50	10,840	140	Peat bog development, minimum-limiting
	AR0719	272	Wood	OS-63272	9630	50	10.980	120	age for recession from the PB3 moraine
Peninsula Avellaneda	AR0620	530–531	Wood fragments	OS-58278	10,050	35	11,560	110	Peat bog development, minimum-limiting age of PB1 moraine
	AR0620	532–533	Twigs	OS-58495	10,250	65	12,000	150	
	AR0620	536–537	Twigs	OS-64829	10,250	40	11,990	90	
	AR0620	537–538	Organic sediment	OS-58557	10,550	55	12,490	80	

(*continued on next page*)

Table A1 (*continued*)

Location	Core	Depth (cm)	Sample description	^{14}C Lab #	^{14}C age	±1σ	Cal yrs	±1σ	Age significance
	AR0622	551	Wood fragments	OS-64992	9740	50	11,160	80	
	AR0622	561–562	Bulk peat	OS-64972	10,200	50	11,900	100	
	AR0623	286–287	Sedge fragments	OS-64963	9620	45	10,970	120	Peat bog development, minimum-limiting
	AR0720b	308	Sedge fragments	OS-65010	10,450	50	12,350	120	age of PB2 moraine
Brazo Rico, Spillway A Site A	AR0518	530–531	Wood	OS-51568	9820	70	11,250	90	Minimum age of spillway abandonment
	AR0518	530–531	Carex seeds	OS-51582	10,100	80	11,680	190	
	AR0519	532–533	Wood	OS51566	9910	55	11,350	100	
	AR0519	532–533	Carex seeds	OS-51570	9990	70	11,490	150	
	AR0520	529–530	Plant stems	OS-53251	10,100	60	11,690	160	
Brazo Rico, Spillway M Site M	AR0503	176–177	Organic sediment*	OS-52108	10,000	45	11480	120	Minimum age of spillway abandonment
	AR0504	264–266	Plant fragments*	OS-64830	10,450	40	12,360	120	
	AR0504	264–266	Plant fragments*	OS-64831	10,500	50	12,450	100	
	AR0504	266–268	Plant stems*	OS-51564	10,500	65	12,420	120	
	AR0504	266–268	Plant fragments*	OS-64839	10,650	45	12,600	40	
	AR0504	266–268	Plant fragments*	OS-64840	10,550	55	12490	80	

Location	Core	Depth (cm)	Sample description	^{14}C Lab #	^{14}C age	±1σ	Cal yrs	±1σ	Age significance
Brazo Rico, Spillway M Site M (cont.)	AR0504	266–268	Plant fragments*	OS-64840	10,550	55	12490	80	Minimum age of spillway abandonment
	AR0504	266–268	Plant fragments*	OS-64841	10,700	45	12,630	40	
	AR0504	278–279	Plant stems*	OS-53565	9150	160	10,340	230	
	AR0504	279–281	Organic fine sand*	OS-64983	10,550	40	12,510	60	
	AR0504	281–283	Plant fragments*	OS-64825	10,200	45	11,900	90	
	AR0505	174–175	Bark-wood fragments	OS-64842	9330	40	10,540	60	Peat development
	AR0505	174–175	Bark-wood fragments	OS-64552	9360	55	10,580	80	
	AR0505	277–278	Plant fragments*	OS-64971	10,650	45	12,600	40	Minimum age of spillway abandonment
	AR0505	277–278	Wood fragments	OS-64553	10,750	75	12,660	70	
	AR0505	289–290	Bryophyte plant fragments	OS-64967	10,450	65	12,340	130	
	AR0505	289–290	Bryophyte plant fragments	OS-64970	10,400	40	12,270	100	
	AR0505	290–291	Sedge macrofossils*	OS-51727	10,500	55	12,440	110	
	AR0505	290–291	Organic fine sand*	OS-64962	10,900	60	12,780	90	
	AR0506	283–284	Sedge fragments*	OS-64526	10,250	50	11,990	110	
	AR0506	284–285	Bark-wood fragments	OS-64525	10,450	55	12,350	130	
	AR0506	284–285	Bark-wood fragments	OS-64551	10,300	50	12,120	130	
	AR0506	284–285	Wood fragments	OS-64550	10,200	50	11,900	100	
	AR0506	285–286	Plant stems*	OS-51728	10,100	55	11,690	160	
	AR0506	285–286	Organic sediment*	OS-64668	10,000	70	11,510	150	
	AR0508	165–166	Wood	OS-51565	10,000	70	11,510	150	
Brazo Rico, Spillway O Site O	AR0516	178–179	Organic sediment	OS-51981	9780	55	11,200	60	Minimum age of spillway abandonment
	AR0517	174–175	Organic sediment	OS-51729	10,050	45	11,570	130	
	AR0517	165–166	Organic sediment	OS-51726	9080	50	10,250	50	Peat development
Bahía Catalana	AR0525	358–359	Organic sediment	OS-51734	10,300	60	12,120	140	Minimum age of spillway abandonment
	AR0525	358–359	Organic sediment	OS-64542	10,100	55	11,690	160	
	AR0525	358–359	Organic sediment	OS-64539	10,200	65	11,890	140	
	AR0526	346–347	Organic sediment	OS-64543	10,000	50	11,490	120	
	AR0526	346–347	Organic sediment	OS-64544	10,100	55	11,690	160	
	AR0526	347–348	Plant fragments	OS-51735	10,200	50	11,900	100	

Location	Core	Depth (cm)	Sample description	^{14}C Lab #	^{14}C age	±1σ	Cal yrs	±1σ	Age significance
Bahía Catalana (cont.)	AR0526	347–348	Organic sediment	OS-51956	10,300	70	12,120	160	Minimum age of spillway abandonment
	AR0527	350–351	Organic sediment	OS-64540	9970	55	11,440	120	
	AR0527	350–351	Organic sediment	OS-64529	10,200	65	11,890	140	
	AR0527	350–351	Organic sediment	OS-51736	10,400	50	12,280	110	
Herminita moraines	AR0613	571–572	Organic sediment	OS-64990	9950	55	11,410	120	Peat bog development, minimum age of Herminita moraines
	AR0613	575–576	Organic sediment	OS-58594	10,350	45	12,220	110	
	AR0704	535	Plant fragments	OS-65004	9290	35	10,480	60	
	AR0705	439	Plant fragments	OS-65005	8920	45	10,050	90	
	AR0714	270	Organic sediment	OS-65007	9960	50	11,420	120	
	AR0614	318–319	Bulk peat	OS-64991	8810	40	9870	120	
	AR0614	321–322	Plant fragments	OS-58493	8530	45	9510	20	
Lago Frías	AR0723	258	Organic sediment	OS-64999	10,400	40	12,270	100	Basal peat immediately outboard of the Neoglacial moraines
Lago Pearson (Anita)	AR0608	223	Sedge fragments	OS-64966	9040	45	10,210	50	
Agassiz Este	LA0704		Wood fragment	OS-63465	8160	60	9130	90	Wood in diamicton below glacigenic units
	AR0616		Wood fragment	OS-58599	8290	40	9300	80	
	AR0717		Wood fragment	OS-58601	8210	35	9170	70	

Notes: Cores from Spillway M, site M (AR0504, AR0505 and AR0506) contained carbonaceous marl-like deposits at depths close to or around samples selected for AMS dating. As a precaution against the possible contamination of some of these samples from hard-water effects, AMS samples originating from aquatic plant remains or bulk sediment that might have been influenced by organically precipitated carbonate have been removed from consideration for chronology development. These samples are indicated by asterisks (*) in the 'sample description' column. Samples originating from terrestrial origin including wood, twigs, and moss fragments are considered to provide robust age estimates at this site.

silty-to-sandy matrix. Lower contacts are sharp, erosive, planar, and tilt largely toward the former ice margin. In Facies D_1 small disturbed sand-and gravel enclaves (Facies B and C) are present.

Genetic interpretation: glacier advance overriding, eroding, and in places including lenses of marginal outwash sediments. Subglacial lodgment till, in places topped by supraglacial till (flow till).

Facies E

Coarse gravelly-to-silty, matrix-supported diamicton. It includes some boulders. The basal contact of the unit is sharp and rests on moraine slopes.

Genetic interpretation: postglacial debris flow generated by slumps on deglaciated moraine slopes.

Tephra:. Genetic interpretation: fallout tephra deposited subaerially or in a calm-water pond. In Site 1 an incipient paleosoil developed.

Peat:. Peat capping and intercalated with gravelly/sandy deposits, or included as clasts incorporated in basal lodgment or deformation till.

Genetic interpretation: peat bog, dismantled by glacial readvance and redeposited as clasts in till.

References

Ackert Jr., R.P., Becker, R.A., Singer, B.S., Kurz, M.D., Caffee, M.W., Mickelson, D.M., 2008. Patagonian glacier response during the late glacial-Holocene transition. Science 321, 392–395.

Anderson, R.F., Ali, S., Bradtmiller, L.I., Nielsen, S.H.H., Fleisher, M.Q., Anderson, B.E., Burckle, L.H., 2009. Wind-driven upwelling in the Southern Ocean and the deglacial rise in atmospheric CO_2. Science 323 (5920), 1443–1448.

Barker, S., Diz, P., Vautravers, M.J., Pike, J., Knorr, G., Hall, I.R., Broecker, W.S., 2009. Interhemispheric Atlantic seesaw response during the last deglaciation. Nature 457 (7233), 1097–1102.

Bronk Ramsay, C., 2010. OxCal 4.1 Manual. OxCal Program 4.1.

Caldenius, C., 1932. Las glaciaciones cuaternarias en la Patagonia y Tierra del Fuego. Ministerio de Agricultura. Dirección General de Minas y Geología, 95–150 (Buenos Aires).

Calvo, E., Pelejero, C., De Deckker, P., Logan, G.A., 2007. Antarctic deglacial pattern in a 30 kyr record of sea surface temperature offshore South Australia. Geophysical Research Letters 34 (13), L13707.

Casassa, G., Rivera, A., 1999. Topografic mass balance model for the Southern Patagonian Icefield, Abstract International Symposium on the Verification of Criospheric models, Bringing Data and Modeling Scientists Together, 16–20 August 1999, Zurich, p.44.

Casassa, G., Rivera, A., Aniya, M., Naruse, R., 2000. Características glaciológicas del Cmpo de Hielo Patagónico Sur. Anales Instituto Patagonia, Serie Cs. Nat 28, 5–22.

Carrasco, J.F., Casassa, G., y Rivera, A., 1998. Climatología actual del Campo de Hielo Sur y posibles cambios por incremento del efecto invernadero, Anales del Instituto de la Patagonia. Serie Ciencias Naturales 26, 119–128.

Denton, G.H., Anderson, R.F., Toggweiler, J.R., Edwards, R.L., Schaefer, J.M., Putnam, A.E., 2010. The last glacial termination. Science 328, 1652–1656.

Denton, G.H., Hendy, C.H., 1994. Younger Dryas age advance of Franz Josef glacier in the southern Alps of New Zealand. Science 264 (5164), 1434–1437.

Feruglio, E., 1944. Estudios geológicos y glaciológicos en la región del Lago Argentino, vol. 37. Boletín Academia Nacional de Ciencias, Córdoba, Argentina (Patagonia)1–208.

Heusser, C.J., 1989. Polar perspective of Late-Quaternary climates in the southern-hemisphere. Quaternary Research 32 (1), 60–71.

Hulton, N.R.J., Purves, R.S., McCulloch, R.D., Sugden, D.E., Bentley, M.J., 2002. The last glacial maximum and deglaciation in southern South America. Quaternary Science Reviews 21, 233–241.

Kaiser, J., Lamy, F., Hebbeln, D., 2005. A 70-kyr sea surface temperature record off southern Chile (Ocean Drilling Program Site 1233). Paleoceanography 20 (4), PA4009. doi:10.1029/2005PA001146.

Kaplan, M.R., Ackert, R.P., Singer, B.S., Douglass, D.C., Kurz, M.D., 2004. Cosmogenic nuclide chronology of millennial-scale glacial advances during O-isotope Stage 2 in Patagonia. Geological Society of America Bulletin 116, 308–321.

Kaplan, M.R., Douglass, D.C., Singer, B.S., Ackert, R.P., Caffee, M.W., 2005. Cosmogenic nuclide chronology of pre-last glacial maximum moraines at Lago Buenos Aires, 46°S, Argentina. Quaternary Research 63, 301–315.

Kaplan, M.R., Schaefer, J.M., Denton, G.H., Barrell, D.J.A., Chinn, T.J.H., Putnam, A.E., Andersen, B.G., Finkel, R.C., Schwartz, R., Doughty, A.M., 2010. Glacier retreat in New Zealand during the younger Dryas stadial. Nature.

King, A.L., Howard, W.R., 2005. delta O-18 seasonality of planktonic foraminifera from Southern Ocean sediment traps: latitudinal gradients and implications for paleoclimate reconstructions. Marine Micropaleontology 56 (1–2), 1–24.

Lamy, F., Kaiser, J., Ninnemann, U., Hebbeln, D., Arz, H.W., Stoner, J., 2004. Antarctic timing of surface water changes off Chile and Patagonian ice sheet response. Science 304 (5679), 1959–1962.

Lamy, F., Kaiser, J., Arz, H.W., Hebbeln, D., Ninnemann, U., Timm, O., Timmermann, A., Toggweiler, J.R., 2007. Modulation of the bipolar seesaw in the southeast Pacific during Termination 1. Earth and Planetary Science Letters 259, 400–413.

Lemieux-Dudon, B., Blayo, E., Petit, J.-R., Waelbroeck, C., Svensson, A., Ritz, C., Barnola, J.-M., Narcisi, B.M., Parrenin, F., 2010. Consistent dating for Antarctic and Greenland ice cores. Quaternary Science Reviews 29 (1–2), 8–20.

Malagnino, E.C., 1995. The Discovery of the Oldest Extra-Andean Glaciation in the Lago Buenos Aires Basin, Argentina. Quaternary of South America and Antarctic Peninsula. A.A. Balkema, Rotterdam (1991): pp. 69–83.

Malagnino, E.C., Strelin, J.A., 1992. Variations of Upsala Glacier in southern Patagonia since the late Holocene to the present. In: Naruse, R., Aniya, M. (Eds.), Glaciological Researches in Patagonia, 1990. Japanese Society of Snow and Ice, pp. 61–85.

McCulloch, R.D., Bentley, M.J., Purves, R.S., Sugden, D.E., Clapperton, C., Hulton, N.R.J., 2000. Climatic inferences from glacial and palaeoecological evidence at the last glacial termination, southern South America. Journal of Quaternary Science 15, 409–418.

Mercer, J.H., 1965. Glacier variations in southern Patagonia. Geographical Review 55, 390–413.

Mercer, J.H., 1970. Variations of some Patagonian glaciers since the late glacial: II. American Journal of Science 269, 1–25.

Mercer, J.H., 1968. Variations of some Patagonian glaciers since the late glacial: I. American Journal of Science 266, 91–109.

Mercer, J.H., 1976. Glacial history of southernmost South America. Quaternary Research 6, 125–166.

Mercer, J.H., Fleck, R.J., Mankinen, E.A., Sander, W., 1975. Southern Patagonia: Glacial Events Between 4 m.y. and 1 m.y. Ago. In: Suggate, R.P., Creswell, M.M. (Eds.), Quaternary Studies. The Royal Society of New Zealand, Wellington, pp. 223–230.

Mercer, J.H., Ager, T., 1983. Glacial and floral changes in Southern Argentina since 14,000 years ago. National Geographic Society Research Reports 15, 457–477.

Monnin, E., Indermühle, A., Dällenbach, A., Flückiger, J., Stauffer, B., Stocker, T.F., Raynaud, D., Barnola, J.-M., 2001. Atmospheric CO_2 concentrations over the Last Glacial Termination. Science 291, 112–114.

Mörner, N.A., Sylwan, C., 1989. Magnetostratigraphy of the Patagonian moraine sequence at Lago Buenos Aires. Journal of South American Earth Sciences 2, 385–390.

Mollenhauer, G., Kienast, M., Lamy, F., Meggers, H., Schneider, R.R., Hayes, J.M., Eglinton, T.I., 2005. An evaluation of C-14 age relationships between co-occurring foraminifera, alkenones, and total organic carbon in continental margin sediments. Paleoceanography 20, PA1016.

Moreno, P.I., Lowell, T.V., Jacobson Jr., G.L., Denton, G.H., 1999. Abrupt vegetation and climate changes during the last glacial maximum and last termination in the Chilean Lake District: a case study from Canal de la Puntilla (41°S). Geografiska Annaler 81A (2), 285–311.

Putnam, A.E., Denton, G.H., Schaefer, J.M., Barrell, D.J.A., Andersen, B.G., Finkel, R.C., Schwartz, R., Doughty, A.M., Kaplan, M.R., Schlüchter, C., 2010. Glacier advance in southern middle latitudes during the Antarctic Cold Reversal. Nature Geoscience 3, 700–704.

Reimer, P., et al., 2009. INTCAL09 and MARINE09 radiocarbon age calibration curves, 0-50,000 years cal BP. Radiocarbon 51, 1111–1150.

Riccardi, A.C., Rolleri, E.O., 1980. Cordillera Patagónica Austral. In: En Turner, J.C. (Ed.), Segundo Simposio de Geología Regional Argentina, vol. 2. Academia Nacional de Ciencias, Córdoba, pp. 1163–1306.

Rodbell, D.T., Smith, J.A., Mark, B.G., 2010. Glaciation in the Andes during the Lateglacial and Holocene. Quaternary Science Reviews 28, 2165–2212.

Roethlisberger, F., 1986. 10.000 Jahre Gletschergeschichte der Erde, vol. 1. Verlag Sauerländer, Aarau, Frankfurt/M., Salzburg. 416.

Sikes, E.L., Howard, W.R., Samson, C.R., Mahan, T.S., Robertson, L.G., Volkman, J.K., 2009. Southern Ocean seasonal temperature and Subtropical Front movement on the South Tasman Rise in the late Quaternary. Paleoceanography 24, PA2201.

Singer, B.S., Ackert, R.P., Guillou, H., 2004. 40Ar/39Ar and K-Ar chronology of Pleistocene glaciations in Patagonia. Geological Society of America Bulletin 116, 434–450.

Strelin, J.A., Malagnino, E.C., 1996. Glaciaciones Pleistocenas de Lago Argentino y Alto Valle del Río Santa Cruz. XIII Congreso Geológico Argentino 4, 311–325.

Strelin, J.A., Malagnino, E.C., 2000. The late-glacial history of Lago Argentino, Argentina, and age of the Puerto Bandera moraines. Quaternary Research 54, 339–347.

Strelin, J.A., Denton, G.H., 2005. Las morenas de Puerto Bandera. XVI Congreso Geológico Argentino y IV Congreso de Exploración de Hidrocarburos. Actas 4, 129–134 (La Plata).

Talley, L.D., 2008. Freshwater transport estimates and the global overturning circulation: shallow, deep and throughflow components. Progress in Oceanography 78 (4), 257–303.

Turney, C.S.M., Roberts, R.G., de Jonge, N., Prior, C., Wilmshurst, J.M., McGlone, M.S., Cooper, J., 2007. Redating the advance of the New Zealand Franz Josef glacier during the last termination: evidence for asynchronous climate change. Quaternary Science Reviews 26, 3037–3042.

Wenzens, G., 2002. The influence of tectonically derived relief and climate on the extent of the last Glaciation east of the Patagonian Icefields (Argentina, Chile). Tectonophysics 345, 329–344.